

FINAL Report D

TRyy1110

**Project Title: Design and Evaluation of High-Volume
Fly Ash (HVFA) Concrete Mixes**

**Report D: Creep, Shrinkage, and Abrasion Resistance of
HVFA Concrete**

Prepared for
Missouri Department of Transportation
Construction and Materials

Missouri University of Science and Technology, Rolla, Missouri

October 2012

The opinions, findings, and conclusions expressed in this publication are those of the principal investigators and the Missouri Department of Transportation. They are not necessarily those of the U.S. Department of Transportation, Federal Highway Administration. This report does not constitute a standard or regulation.

ABSTRACT

The main objective of this study was to determine the effect on shrinkage, creep, and abrasion resistance of high-volume fly ash (HVFA) concrete. The HVFA concrete test program consisted of comparing the shrinkage, creep, and abrasion performance of two concrete mix designs with 70% cement replacement with Class C fly ash relative to a Missouri Department of Transportation (MoDOT) standard mix design.

Modified versions of standard test methods were used for the shrinkage and creep portions of the study. Shrinkage was measured through a modified version of ASTM C157 “Standard Test Method for Length Change of Hardened Hydraulic-Cement Mortar and Concrete,” while creep was measured through a modified version of ASTM C512 “Standard Test Method for Creep of Concrete in Compression.” Abrasion resistance was measured in accordance with ASTM C944 “Standard Test Method for Abrasion Resistance of Concrete or Mortar Surfaces by Rotating-Cutter Method.”

In addition to comparisons between the three mix designs, the results were also compared to existing prediction models and previous research results on HVFA concrete. Both HVFA concrete mixes showed a significant decrease in shrinkage strain relative to the control concrete, which was very consistent with previous research. With regard to creep, both HVFA concrete mixes also showed improved performance over the control mix, again confirming previous research results. However, the control concrete exhibited improved abrasion resistance relative to the two HVFA concrete mixes, which coincided with the higher strength of the control mix. At later ages, the abrasion resistance of the HVFA concrete improved due to late age strength gain characteristic of this material.

TABLE OF CONTENTS

	Page
ABSTRACT	ii
LIST OF ILLUSTRATIONS.....	vi
LIST OF TABLES.....	viii
NOMENCLATURE	ix
1. LITERATURE REVIEW.....	1
1.1. HIGH VOLUME FLY ASH CONCRETE (HVFA)	1
1.1.1. Fly Ash.	1
1.1.2. Definition of HFVA.	1
1.1.3. Advantages of HVFA.....	2
1.2. SHRINKAGE OF CONCRETE	2
1.2.1. Definition of Shrinkage.....	2
1.2.2. Factors Affecting Shrinkage (ACI 209.1R-05).....	3
1.3. SHRINKAGE MODELS.....	5
1.3.1. ACI 209R-92.	5
1.3.2. NCHRP Report 496 (2003).....	9
1.3.3. Model B3.....	11
1.3.4. CEB-FIP 90.....	12
1.3.5. GL 2000.....	13
1.4. HVFA SHRINKAGE RESEARCH.....	14
1.4.1. Atis.	15
1.4.2. Termkhajornkit, et. al.	16
1.4.3. Gao, et. al.....	16
1.4.4. Nath and Sarker.....	17
1.5. CREEP OF CONCRETE.....	18
1.5.1. Definition of Creep.....	18
1.5.2. Factors Affecting Creep.	19
1.6. CREEP MODELS.....	20

1.6.1. ACI 209R-92.....	20
1.6.2. NCHRP Report 496.....	21
1.6.3. CEB-FIP 90.....	23
1.6.4. GL 2000.....	24
1.7. HVFA CREEP RESEARCH	24
1.7.1. ACI 232.2R-03.....	24
1.7.2. Alexander, et. al.....	25
1.8. APPLICATION OF SHRINKAGE AND CREEP.....	25
1.8.1. Prestress Loss.....	25
1.8.2. Load Effects.....	26
1.8.3. Beam Deflection.....	27
1.9. CONCRETE ABRASION	27
1.9.1. Definition of Concrete Abrasion.....	27
1.9.2. Factors Affecting Concrete Abrasion.....	28
1.10. HVFA ABRASION RESEARCH	28
1.10.1. Naik, et. al.....	28
1.10.2. Atis.....	29
2. RESEARCH PROGRAM	30
2.1. MIX DESIGNS.....	30
2.1.1. HVFA.....	30
2.2. SHRINKAGE AND CREEP SPECIMEN CONSTRUCTION.....	31
2.2.1. Shrinkage and Creep Specimens.....	31
2.2.2. Shrinkage and Creep Molds.....	31
2.2.3. Shrinkage and Creep Specimen Casting.....	32
2.2.4. Shrinkage and Creep De-Molding and Preparation.....	33
2.2.5. Shrinkage and Creep Data Acquisition.....	33
2.3. ABRASION SPECIMEN CONSTRUCTION	34
2.4. TESTING PROCEDURES.....	35
2.4.1. Shrinkage Testing Procedures.....	35
2.4.2. Creep Testing Procedures.....	38
2.4.3. Abrasion Resistance Testing Procedures.....	41

3. HVFA RESULTS AND DISCUSSION.....	45
3.1. SHRINKAGE	45
3.1.1. Results.	45
3.1.2. Conclusions and Discussion.	45
3.2. CREEP	53
3.2.1. Results.	53
3.2.2. Discussion and Conclusions.	53
3.3. ABRASION RESISTANCE.....	54
3.3.1. Results.	54
3.3.2. Discussion and Conclusions.	58
APPENDIX A.....	60
APPENDIX B.....	64
APPENDIX C.....	67
BIBLIOGRAPHY.....	70

LIST OF ILLUSTRATIONS

Figure	Page
Figure 1.1 - Relationship Between Moist Cure Time and Shrinkage Strain	4
Figure 1.2 - Series A Shrinkage Results (adapted from Nath and Sarker)	17
Figure 1.3 - Series B Shrinkage Results (adapted from Nath and Sarker)	18
Figure 1.4 - Stress vs. Time for Prestressed Bridge Girder (Tadros et. al. 2003).....	26
Figure 2.1 - Shrinkage and Creep Form.....	32
Figure 2.2 – Shrinkage and Creep Specimens and DEMEC Point Arrangement (Myers and Yang, 2005)	34
Figure 2.3 – DEMEC Reading Taken on Specimen	36
Figure 2.4 - Reference Bar	36
Figure 2.5 - Reading Taken on Reference Bar	37
Figure 2.6 - Gauge Factor Used for Shrinkage and Creep Calculations.....	37
Figure 2.7 - Example DEMEC Gauge Reading.....	37
Figure 2.8 - Schematic of Creep Loading Frame (Myers and Yang, 2005)	38
Figure 2.9 - Creep Loading Frame with Specimen.....	39
Figure 2.10 - Reading Taken on Creep Specimen	40
Figure 2.11 - Schematic of Abrasion Rotating Cutter (ASTM C944).....	42
Figure 2.12 - Rotating Cutter	42
Figure 2.13 - Abrasion Resistance Test In Progress	43
Figure 2.14 - Depth of Wear Measurement Points	43
Figure 2.15 - Abrasion Resistance Specimen After Testing.....	44
Figure 3.1 - HVFA-C Shrinkage Results and Prediction Models.....	46

Figure 3.2 - HVFA-H Shrinkage Results and Prediction Models	47
Figure 3.3 - HVFA-L Shrinkage Results and Prediction Models	48
Figure 3.4 – HVFA Shrinkage Results (Best fit Logarithmic)	49
Figure 3.5 – HVFA Shrinkage Results Compared to Marlay (2011)	50
Figure 3.6 – HVFA Shrinkage Results Compared to Atis (2003)	51
Figure 3.7 – HVFA Results with Shrinkage Databases	52
Figure 3.8 - HVFA-C Mass Loss Results	55
Figure 3.9 - HVFA-H Mass Loss Results	55
Figure 3.10 - HVFA-L Mass Loss Results	56
Figure 3.11 - HVFA Average Depth of Wear by Age	56
Figure 3.12 - HVFA Average Mass Loss by Age	57
Figure 3.13 - HVFA Mass Loss Results	57
Figure 3.14 - HVFA Depth of Wear Results	58

LIST OF TABLES

Table	Page
Table 1.1 - Standard Conditions as Defined by ACI 209R-92	7
Table 1.2 - Mix Designs (Atis 2003) (kg per cubic meter).....	15
Table 1.3 - Experimental Shrinkage Results (Atis 2003) (microstrain)	16
Table 2.1 - HVFA Test Program Mix Designs and mechanical properties	31
Table 3.1 - Summary of HVFA Creep Results	53
Table 3.2 - Average Mass Loss Shown with 28 Day Compressive Strength	58

NOMENCLATURE

Symbol	Description
A	Cement type correction factor (NCHRP 628)
A_c	Cross-section area (mm^2) (CEB-FIP 90)
c	Cement content (lb/yd^3) (ACI 209R-92)
D	Effective cross-section thickness (Model B3)
D_0	Datum reading on the reference bar
D_i	Subsequent reading on the reference bar
f	Size effects factor (ACI 209R-92)
f'_c	Tested compressive strength of concrete (psi, ksi, MPa)
f'_{ci}	Specified compressive strength of concrete (ksi) (NCHRP 496)
f_{cm}	Tested compressive strength of concrete at 28 days age (psi, ksi, MPa) (CEB-FIP 90)
G	Gauge factor
H	Relative humidity (% or decimal)
K	Cement type correction factor (GL 2000)
k_f	Concrete strength factor (NCHRP 496)
k_{hc}	Humidity factor (NCHRP 496)
k_{hs}	Humidity factor (NCHRP 496 and NCHRP 628)
k_{la}	Loading factor (NCHRP 496)
k_s	Size factor (NCHRP 496 and NCHRP 628) or Cross-section shape factor (Model B3)
k_{td}	Time development factor (NCHRP 496)

R_0	Datum reading on tested material
RH	Relative humidity (%) (CEB-FIP 90)
R_i	Subsequent reading on tested material
s	Slump of fresh concrete (in)
S(t)	Time dependence factor (Model B3)
t	Age of concrete (days)
t_0	Age of concrete when drying begins (days) (Model B3) or Age at which creep specimen is loaded (days) (ACI 209R-92 and CEB FIP 90)
t_c	Age of concrete when drying begins (days) (ACI 209R-92 and GL 2000)
t_i	Age at which creep specimen is loaded (days) (NCHRP 496)
t_s	Age of concrete at the beginning of shrinkage (days) (CEB-FIP 90)
u	Perimeter in contact with the atmosphere (mm) (CEB-FIP 90)
V/S	Volume to Surface area ratio (in or mm)
w	Water content of concrete (lb/ft ³)
α	Concrete air content (%)
α_1	Cement type correction factor (Model B3)
α_2	Curing condition correction factor
$\beta(h)$	Humidity correction factor (GL 2000)
$\beta(t)$	Time effect correction factor (GL 2000)
β_c	Coefficient to describe the development of creep with time after loading (CEB FIP 90)

β_{RH}	Relative humidity correction factor (CEB-FIP 90)
β_s	Coefficient to describe the development of shrinkage with time (CEB-FIP 90)
β_{sc}	Concrete type correction factor (CEB-FIP 90)
$\gamma_{c,RH}$	Humidity correction factor (ACI 209R-92)
$\gamma_{c,s}$	Slump correction factor (ACI 209R-92)
$\gamma_{c,t0}$	Curing condition correction factor (ACI 209R-92)
$\gamma_{c,vs}$	Size correction factor (ACI 209R-92)
$\gamma_{c,\alpha}$	Air content correction factor (ACI 209R-92)
$\gamma_{c,\psi}$	Fine aggregate correction factor (ACI 209R-92)
$\gamma_{sh,c}$	Cement content correction factor (ACI 209R-92)
$\gamma_{sh,RH}$	Relative humidity correction factor (ACI 209R-92)
$\gamma_{sh,s}$	Slump correction factor (ACI 209R-92)
$\gamma_{sh,tc}$	Initial moist cure duration correction factor (ACI 209R-92)
$sh_{,vs}$	Volume/surface area correction factor (ACI 209R-92)
$\gamma_{sh,\alpha}$	Air content correction factor (ACI 209R-92)
$\gamma_{sh,\psi}$	Fine aggregate correction factor (ACI 209R-92)
Δ_{ϵ_c}	Change in creep strain from one reading to the next
Δ_{ϵ_s}	Change in shrinkage strain from one reading to the next
ϵ_{cso}	Notional shrinkage coefficient (CEB-FIP 90)
$\epsilon_{es(t,ts)}$	Calculated ultimate shrinkage strain ($\mu\epsilon$) (CEB-FIP 90)
ϵ_i	Measured strain due to initial loading of creep specimen
$\epsilon_{es(t,t0)}$	Calculated shrinkage strain at a given age ($\mu\epsilon$) (Model B3)

ϵ_{sh}	Calculated shrinkage strain at a given age ($\mu\epsilon$) (NCHRP 496, GL 2000, and NCHRP 628)
$\epsilon_{sh(t,tc)}$	Calculated shrinkage strain at a given age ($\mu\epsilon$) (ACI 209R-92)
ϵ_{shu}	Calculated ultimate shrinkage strain ($\mu\epsilon$) (ACI 209R-92) or Notional ultimate shrinkage strain (GL 2000)
$\epsilon_{sh\infty}$	Calculated ultimate shrinkage strain ($\mu\epsilon$) (Model B3)
ϵ_t	Measured creep strain at a given age
λ_{Δ}	Multiplier for additional deflection due to long-term effects (ACI 318-08)
ξ	Time dependant factor for sustained load (ACI 318-08)
ρ'	Compression reinforcement ratio (ACI 318-08)
τ_{sh}	Size dependence factor (Model B3)
$\Phi_{(t,t_0)}$	Calculated creep coefficient at a given age (ACI 209R-92 and CEB FIP 90) or Measured creep coefficient at a given age
Φ_0	Notional creep coefficient (CEB FIP 90)
Φ_{28}	Calculated creep coefficient at a given age (GL 2000)
$\Phi_{(tc)}$	Factor that takes into account drying before loading (GL 2000)
Φ_u	Calculated ultimate creep coefficient (ACI 209R-92)
Ψ	Ratio of fine aggregate to total aggregate by weight (%)
$\Psi_{(t,t_i)}$	Calculated creep coefficient at a given age (NCHRP 496 and NCHRP 628)

1. LITERATURE REVIEW

1.1. HIGH VOLUME FLY ASH CONCRETE (HVFA)

1.1.1. Fly Ash. Fly ash is defined by ACI 116R-00 as “the finely divided residue that results from the combustion of ground or powdered coal and that is transported by flue gases from the combustion zone to the particle removal system.” Fly ash is often collected in this manner from coal burning electric power plants and is considered a waste product of the power plant. As reported by the American Coal Ash Association’s 2010 Coal Combustion Product Production & Use Survey Report, there were 67,700,000 tons (61,400,000,000 kg) of fly ash produced, of which 11,000,000 tons (9,990,000,000 kg) (16.3%) were used in concrete, concrete products, or grout.

1.1.2. Definition of HFVA. Concretes containing 15% - 35% fly ash replacement by mass of total cementitious material are typically used. High volume concrete is concrete that contains a much higher percentage of fly ash replacement than the typical fly ash concrete mix. The exact definition of high volume fly ash concrete varies depending on the source. ACI 232.2R-03 states “HVFA concrete may be defined as having a fly ash content of 50% or greater by mass of cementitious materials.” ACI also cites research from Haque, Langan, and Ward (1984) and Ramme and Tharaniyil (2000) which define high volume fly ash concrete as concrete with fly ash replacement of 40% and 37% respectively. The report concludes that “HVFA concrete can be considered to represent concrete containing higher percentages of fly ash than normal for the intended application of the concrete.” (ACI 232.2R-11)

1.1.3. Advantages of HVFA. The advantages of using fly ash as a replacement for Portland cement in concrete production include economic benefits, environmental benefits, as well as some advantageous material properties. Fly ash is generally cheaper to purchase than Portland cement, however this is dependent on local availability and transportation costs. Since fly ash is otherwise considered a waste product, which is either disposed of in landfills or released into the atmosphere, its use as a recycled material is considered very environmentally advantageous. The use of HVFA concrete can contribute to LEED certification by the U.S. Green Building Council, applicable to MR credit 4-recycled content (USGBC). Use of fly ash also has beneficial effects on the properties of the concrete in which it is used. Because fly ash has a lower specific gravity than cement, its replacement by mass will increase the paste volume of the concrete, allowing for an increase in workability. Fly ash also contributes to less bleeding in fresh concrete. HVFA concrete also retards setting time and strength gain, which can be beneficial in mass concrete projects. Research has also shown that fly ash concrete reaches a higher ultimate strength than conventional concrete.

1.2. SHRINKAGE OF CONCRETE

1.2.1. Definition of Shrinkage. Shrinkage of concrete is the decrease in volume of hardened concrete with time. Shrinkage is expressed as the strain measured on a load-free specimen, most often as the dimensionless unit microstrain (strain $\times 10^{-6}$). Concrete experiences shrinkage in three ways, drying shrinkage, autogenous (chemical) shrinkage, and carbonation shrinkage. Autogenous shrinkage is due strictly to the hydration reactions of the cement. Drying shrinkage is the strain imposed on a specimen

exposed to the atmosphere and allowed to dry. Carbonation shrinkage is caused by the reaction of calcium hydroxide with cement with carbon dioxide in the atmosphere. The magnitude and rate of shrinkage is dependent on a number of factors. These factors are accounted for and described in the various industry models and research projects in the following sections.

1.2.2. Factors Affecting Shrinkage (ACI 209.1R-05). Shrinkage of concrete is closely related to shrinkage of paste. Therefore the amount of paste in the mix significantly affects the level of concrete shrinkage. Paste volume is determined by the quantity, size, and gradation of aggregate. Because paste volume is largely dependent on aggregate properties, the most important factor in determining a concrete's shrinkage level is the aggregate used in the mix. Similarly, the water content, cement content, and slump will affect the shrinkage of concrete. These three factors are indications of the paste volume and therefore can be used to determine the shrinkage potential of a mix. Aggregate acts as a restraining force to shrinkage, therefore an aggregate with a higher modulus of elasticity (MOE) will better restrain against shrinkage than an aggregate with a lower MOE. The characteristics of the cement itself are other significant indicators of shrinkage potential. Research has shown cements with low sulfate content, high alumina content, and cements that are finely ground exhibit increased shrinkage.

The environment which the concrete is exposed to can also influence shrinkage. The biggest environmental factor is the relative humidity of the surrounding air. As shown by **Eq. 2.1**, as relative humidity increases, shrinkage decreases due to the decrease in potential moisture loss. It has also been shown that an increase in temperature increases the ultimate shrinkage of concrete.

$$\text{shrinkage} \propto 1 - \left(\frac{h}{100}\right)^b \quad (1.1)$$

Where: h is relative humidity in percent, and b is a constant that ranges from 1 to 4.

Finally, the design and construction of concrete specimens can influence shrinkage. The curing conditions experienced by the concrete have a significant effect on shrinkage. Generally, the longer the specimen is allowed to moist cure, the less it will shrink. However, research conducted by Perenchio (1997), **Figure 1.1**, shows that there may not be a simple relationship between moist cure time and shrinkage.

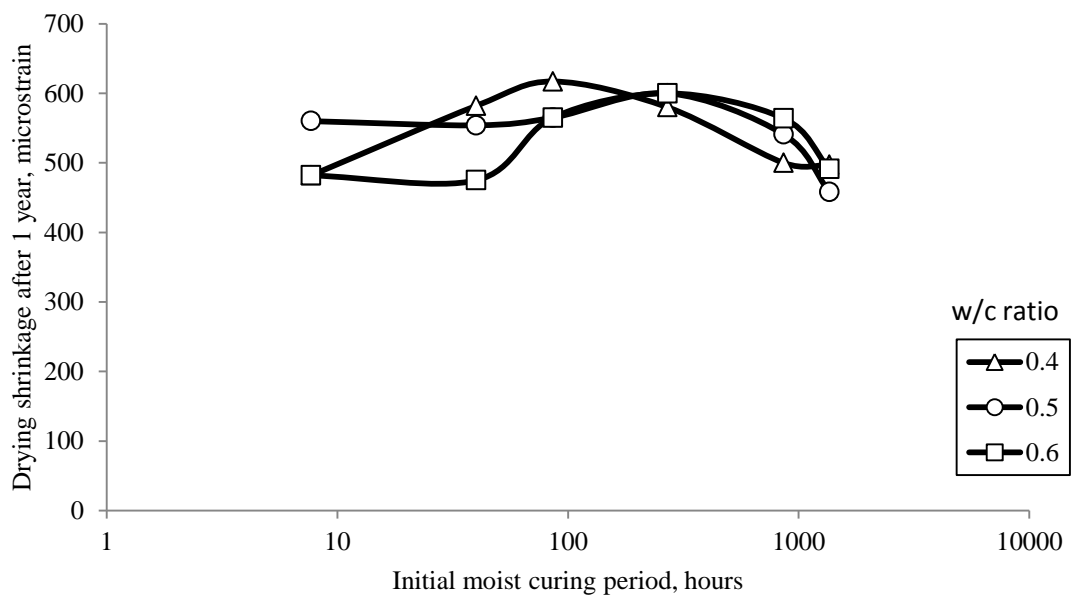


Figure 1.1 - Relationship Between Moist Cure Time and Shrinkage Strain (adapted from Perenchio 1997)

Larger members tend to dry slower, so the ratio of volume to surface area is a significant factor in shrinkage of concrete.

$$\text{shrinkage} \propto \frac{1}{\left(\frac{V}{S}\right)^2} \quad (1.2)$$

Where: V/S is the volume to surface area ratio in inches.

1.3. SHRINKAGE MODELS.

The ability to accurately predict the shrinkage of a concrete structure is extremely important. An accurate model for shrinkage will allow the engineer to predict long term serviceability, durability, and stability of a given structure. As mentioned above, there are many different factors that affect a concrete's susceptibility to shrinkage. Because of these factors, accurate prediction of shrinkage is very difficult. The models described below take into account many of the factors described above in their attempt to predict concrete shrinkage (Bazant and Baweja, 2000).

1.3.1. ACI 209R-92. This model, developed by Branson and Christiason (1971) and modified by ACI committee 209, predicts shrinkage strain of concrete at a given age under standard conditions. The original model by Branson and Christiason was developed based on a best fit from a sample of 95 shrinkage specimens and using an ultimate shrinkage strain of 800×10^{-6} in./in. (mm/mm). However, subsequent research by Branson and Chen, based on a sample of 356 shrinkage data points, concluded that the ultimate shrinkage strain should be 780×10^{-6} in./in. (mm/mm). The prediction model, **Eq. 1.3 – 1.5**, apply only to the standard conditions as shown in **Table 1.1**.

$$\varepsilon_{sh}(t, t_c) = \frac{(t-t_c)^\alpha}{f+(t-t_c)^\alpha} \varepsilon_{shu} \quad (\mu\varepsilon) \quad (1.3)$$

$$\varepsilon_{shu} = 780 \times 10^{-6} \quad (\mu\varepsilon) \quad (1.4)$$

$$f = 26.0e^{\{0.36(V/S)\}} \quad (1.5)$$

Where: f is 35 (moist cure) or 55 (steam cure), or by **Eq. 1.5** if size effects are to be considered, α is assumed to be 1, t is the age of concrete in days, and t_c is the age of concrete when drying begins in days.

Table 1.1 - Standard Conditions as Defined by ACI 209R-92

Factors		Variables		Standard
Concrete	Concrete Composition	Cement Paste Content	Type of Cement	Type I or III
		W/C	Slump	2.7 in (70mm)
		Mix Proportions	Air Content	≤ 6%
		Aggregate Characteristics	Fine Aggregate %	50%
		Degree of Compaction	Cement Content	470 to 752 lb/yd ³ (279 to 446 kg/m ³)
	Initial Curing	Length of Initial Curing	Moist Cured	7 days
			Steam Cured	1 - 3 days
		Curing Temperature	Moist Cured	73.4 ± 4°F (23 ± 2°C)
			Steam Cured	≤ 212°F (≤ 100°C)
		Curing Humidity	Relative Humidity	≥ 95%
Member Geometry & Environment	Environment	Concrete Temperature	Concrete Temperature	73.4°F ± 4°F (23 ± 2°C)
		Concrete Water Content	Ambient Relative Humidity	40%
	Geometry	Size and Shape	Volume-Surface Ratio (V/S)	V/S = 1.5 in (38mm)
			Minimum Thickness	6 in (150mm)

When concrete is not subject to any or all of the standard conditions, correction factors shall be applied, as shown in **Eq. 1.6 – 1.16**.

$$\varepsilon_{sh}(t, t_c) = \frac{(t-t_c)^\alpha}{f+(t-t_c)^\alpha} \times \varepsilon_{shu} \quad (\mu\varepsilon) \quad (1.6)$$

$$f = 26.0e^{\{0.36(V/S)\}} \quad (1.7)$$

$$\varepsilon_{shu} = 780\gamma_{sh} \times 10^{-6} \quad (\mu\varepsilon) \quad (1.8)$$

$$\gamma_{sh} = \gamma_{sh,tc} \gamma_{sh,RH} \gamma_{sh,vs} \gamma_{sh,s} \gamma_{sh,\psi} \gamma_{sh,c} \gamma_{sh,\alpha} \quad (1.9)$$

$$\gamma_{sh,tc} = 1.202 - .2337 \log(t_c) \quad (1.10)$$

$$\gamma_{sh,RH} = \begin{cases} 1.40 - 1.02h & \text{for } 0.40 \leq h \leq 0.80 \\ 3.00 - 3.0h & \text{for } 0.80 \leq h \leq 1 \end{cases} \quad (1.11)$$

$$\gamma_{sh,vs} = 1.2e^{\{-0.12(V/S)\}} \quad (1.12)$$

$$\gamma_{sh,s} = 0.89 + 0.041s \quad (1.13)$$

$$\gamma_{sh,\psi} = \begin{cases} 0.30 + 0.014\psi & \text{for } \psi \leq 50\% \\ 0.90 + 0.002\psi & \text{for } \psi > 50\% \end{cases} \quad (1.14)$$

$$\gamma_{sh,c} = 0.75 + 0.00036c \quad (1.15)$$

$$\gamma_{sh,\alpha} = 0.95 + 0.008\alpha \geq 1 \quad (1.16)$$

Where: $\varepsilon_{sh}(t, t_c)$ is the calculated shrinkage strain at a given age, ε_{shu} is the calculated ultimate shrinkage strain, $\gamma_{sh,tc}$ is the initial moist cure duration correction factor, t is the age of concrete in days, t_c is the age of concrete when drying starts in days, $\gamma_{sh,RH}$ is the relative humidity correction factor, h is humidity in decimals, $\gamma_{sh,vs}$ is the volume/surface

area correction factor, where V/S is the volume to surface area ratio in inches, $\gamma_{sh,s}$ is the slump correction factor, s is slump in inches, $\gamma_{sh,\psi}$ is the fine aggregate correction factor, ψ is the ratio of fine aggregate to total aggregate by weight expressed as percentage, $\gamma_{sh,c}$ is the cement content correction factor, c is the cement content in lb/yd^3 , $\gamma_{sh,\alpha}$ is the air content correction factor, and α is the air content in percent. In **Eq 1.6**, the value of α can be assumed to be equal to 1, with f assumed to be equal to 35 for concrete that is moist cured for seven days or 55 for concrete subject to 1-3 days of steam curing. In order to totally consider shape and size effects, α is still assumed to be equal to 1, with f given by **Eq. 1.7**.

1.3.2. NCHRP Report 496 (2003). The National Cooperative Highway Research Program (NCHRP) conducted research on shrinkage of high strength concrete in the states of Nebraska, New Hampshire, Texas, and Washington. This research project was sponsored by the American Association of State Highway and Transportation Officials (AASHTO) and the results adopted into the 2007 AASHTO LRFD Bridge Design Specifications. Laboratory shrinkage data was obtained from three 4 in. (101.6 mm) by 4 in. (101.6 mm) by 24 in. (609.6 mm) specimens per mix, with a total of 48 specimens tested including both normal and high strength concrete. Field specimens were also made and cured in the same condition as corresponding bridge girders in each of the four participating states. The field program consisted of a set of three 4 in. (101.6 mm) by 4 in. (101.6 mm) by 24 in. (609.6 mm) shrinkage specimens at each location with measurements taken for 3 months. The data showed that an ultimate shrinkage strain of 480×10^{-6} in./in. (mm/mm) should be assumed. The modification factors in the model

account for the effects of high strength concrete. **Eq. 1.17 – 1.22** present the proposed shrinkage formula as proposed in this study.

$$\varepsilon_{sh} = 480 \times 10^{-6} \gamma_{sh} \quad (\mu\varepsilon) \quad (1.17)$$

$$\gamma_{sh} = k_{td} k_s k_{hs} k_f \quad (1.18)$$

$$k_{td} = \frac{t}{61 - 4f'_{ci} + t} \quad (1.19)$$

$$k_{hs} = 2.00 - 0.0143H \quad (1.20)$$

$$k_s = \frac{1064 - 94V/S}{735} \quad (1.21)$$

$$k_f = \frac{5}{1 + f'_{ci}} \quad (1.22)$$

Where: ε_{sh} is the calculated shrinkage strain at a given age, k_{td} is the time development factor, t is the age of the concrete in days, k_{hs} is the humidity factor, H is the average ambient relative humidity in percent, k_s is the size factor, V/S is the volume to surface area ratio in inches, k_f is the concrete strength factor, and f'_{ci} is the specified compressive strength of concrete in ksi.

1.3.3. Model B3. Model B3 (Bazant and Baweja) is the third update of shrinkage predictions developed at Northwestern University, based on BP model β_3 and BP-KX model β_4 . This model is simpler than previous versions and is validated by a larger set of test data. **Eq. 1.23 – 1.32** present the B3 shrinkage prediction model.

$$\varepsilon_{sh}(t, t_0) = -\varepsilon_{sh\infty}k_h S(t) \quad (\mu\varepsilon) \quad (1.23)$$

$$S(t) = \tanh \sqrt{\frac{t-t_0}{\tau_{sh}}} \quad (1.24)$$

$$k_h = \begin{cases} 1 - h^3 & \text{for } h \leq 0.98 \\ -0.2 & \text{for } h = 1 \text{ (swelling in water)} \\ \text{linear} & \\ \text{interpolation} & \text{for } 0.98 \leq h \leq 1 \end{cases} \quad (1.25)$$

$$\tau_{sh} = k_t(k_s D)^2 \quad (1.26)$$

$$k_t = 190.8t_0^{-0.08}f'_c{}^{-1/4} \quad (1.27)$$

$$D = 2V/S \text{ (in.)} \quad (1.28)$$

$$k_s = \begin{cases} 1.00 & \text{for an infinite slab} \\ 1.15 & \text{for an infinite cylinder} \\ 1.25 & \text{for an infinite square prism} \\ 1.30 & \text{for a sphere} \\ 1.55 & \text{for a cube} \end{cases} \quad (1.29)$$

$$\varepsilon_{sh\infty} = -\alpha_1\alpha_2[26w^{2.1}f'_c{}^{-0.28} + 270] \quad (\mu\varepsilon) \quad (1.30)$$

$$\alpha_1 = \begin{array}{ll} 1.0 & \text{for type I cement} \\ 0.85 & \text{for type II cement} \\ 1.1 & \text{for type III cement} \end{array} \quad (1.31)$$

$$\alpha_2 = \begin{array}{ll} 0.75 & \text{for steam – curing} \\ 1.2 & \text{for sealed or normal curing in air} \\ & \text{with initial protection against drying} \\ 1.0 & \text{for curing in water or at 100\% relative humidity} \end{array} \quad (1.32)$$

Where: $\varepsilon_{shu}(t, t_0)$ is the calculated shrinkage strain at a given age, $S(t)$ is the time dependence factor, t is the age of concrete in days, t_0 is the age of concrete at which drying begins, τ_{sh} is the size dependence factor, f'_c is the cylinder compressive strength in psi, D is the effective cross-section thickness, V/S is the volume to surface area ratio in inches, k_s is the cross-section shape factor, $\varepsilon_{sh\infty}$ is the calculated ultimate shrinkage strain, α_1 is the cement type correction factor, α_2 is the curing condition correction factor, and w is the water content of the concrete in lb/ft^3 .

1.3.4. CEB-FIP 90. This model, developed jointly by Euro-International Concrete Committee (CEB – Comité Euro-International du Béton) and the International Federation for Prestressing (FIP – Fédération Internationale de la Précontrainte) is found in the CEB-FIP Model Code 1990. It is stated that due to its international character, the code is more general than most and does not apply to any particular structure type. **Eq. 1.33 – 1.38** present this model for calculating shrinkage strain.

$$\varepsilon_{es}(t, t_s) = \varepsilon_{cso}\beta_s(t - t_s) \quad (\mu\varepsilon) \quad (1.33)$$

$$\varepsilon_{\text{cso}} = \varepsilon_s(f_{\text{cm}})(\beta_{\text{RH}}) \quad (1.34)$$

$$\beta_s(t - t_s) = \sqrt{\frac{(t - t_s)}{350\left(\frac{2A_c}{100u}\right)^2 + (t - t_s)}} \quad (1.35)$$

$$\varepsilon_s(f_{\text{cm}}) = [160 + 10\beta_{\text{sc}}(9 - 0.1f_{\text{cm}})] \times 10^{-6} \quad (1.36)$$

$$\beta_{\text{RH}} = -1.55[1 - (RH/100)^3] \quad (1.37)$$

$$\beta_{\text{sc}} = \begin{cases} 4 & \text{for slowly hardening cements} \\ 5 & \text{for normal or rapid hardening cements} \\ 8 & \text{for rapid hardening high strength cements} \end{cases} \quad (1.38)$$

Where: $\varepsilon_s(t, t_s)$ is the calculated ultimate shrinkage strain, ε_{cso} is the notional shrinkage coefficient, β_s is the coefficient to describe the development of shrinkage with time, t is the age of concrete in days, t_s is the age of concrete at the beginning of shrinkage in days, A_c is the cross section area in mm^2 , u is the perimeter in contact with the atmosphere in mm, f_{cm} is the compressive strength of concrete at age of 28 days in MPa, β_{RH} is the relative humidity correction factor, RH is the relative humidity in percent, and β_{sc} is the concrete type correction factor.

1.3.5. GL 2000. This model, developed by Gardener and Lockman was published in the ACI materials journal under the title “Design provisions for drying shrinkage and Creep of Normal-Strength Concrete.” The model developed is shown in **Eq. 1.39 – 1.43.**

$$\varepsilon_{sh} = \varepsilon_{shu}\beta(h)\beta(t) \quad (\mu\varepsilon) \quad (1.39)$$

$$\varepsilon_{shu} = 1000K\sqrt{\frac{30}{f'_c}} \times 10^{-6} \quad (\mu\varepsilon) \quad (1.40)$$

$$\beta(h) = 1 - 1.18h^4 \quad (1.41)$$

$$\beta(t) = \sqrt{\frac{t-t_c}{t-t_c+0.15(V/S)^2}} \quad (1.42)$$

$$K = \begin{array}{ll} 1 & \text{for type I cement} \\ 0.75 & \text{for type II cement} \\ 1.15 & \text{for type III cement} \end{array} \quad (1.43)$$

Where: ε_{sh} is the calculated shrinkage strain at a given age, ε_{shu} is the notional ultimate shrinkage strain, $\beta(h)$ is the humidity correction factor, h is humidity in decimals, $\beta(t)$ is the correction factor for the effect of time on shrinkage, t_c is the age that drying has commenced in days, t is age of concrete in days, V/S is the volume to surface area ratio, and K is the cement type correction factor.

1.4. HVFA SHRINKAGE RESEARCH

Shrinkage of concrete containing fly ash has been researched extensively. The sections below present the data collected and results compiled from research programs into shrinkage of HVFA concrete.

1.4.1. Atis. Six concrete mixes were tested for shrinkage strain at ages up to 6 months. Two mixes were conventional concrete, two had a fly ash replacement of 70% by mass of cement, and the final two mixes had a fly ash replacement of 50% by mass of cement. The mix designs used in this project are shown in **Table 1.2**. Each pair of mixes (OPC, 70%, and 50%) had one mix which was considered roller compacted concrete (RCC) and had a slump of zero. The other mix contained superplasticizer which produced a mix which was practically flowable. At every age of testing and for each type of mix, RCC and flowable, except at 14 days for the flowable mixes, the measured shrinkage strain decreased as the fly ash replacement percentage increased. The results show that concrete made with superplasticizer showed higher shrinkage strains than concrete made without superplasticizer. It was also concluded that, because of HVFA concrete's lower shrinkage strain, the number of joints in concrete pavement construction could be reduced by the use of HVFA concrete. The experimental results are shown in **Table 1.3**.

Table 1.2 - Mix Designs (Atis 2003) (kg per cubic meter)

Mix	M1	M2	M3	M4	M5	M6
Cement (kg)	400	400	120	120	200	200
Fly ash (kg)	---	---	280	280	200	200
Sand (kg)	600	600	600	600	600	600
Gravel (kg)	1200	1200	1200	1200	1200	1200
Water (L)	136	128	112	116	132	120
Optimum W/C ratio	0.32	0.32	0.29	0.29	0.30	0.30
Actual W/C ratio	0.34	0.32	0.28	0.29	0.33	0.30
Superplasticizer	5.6	---	5.6	---	5.6	---
Flow table (mm)	560	0	570	0	600	0

Conversion: $1 \text{ kg/m}^3 = 1.686 \text{ lb/yd}^3$

Table 1.3 - Experimental Shrinkage Results (Atis 2003) (microstrain)

Drying Time	M1	M2	M3	M4	M5	M6
1 day	86	72	56	34	63	38
3 days	134	122	94	69	109	88
7 days	172	148	144	100	153	113
14 days	225	190	164	141	192	125
28 days	347	265	231	163	256	169
56 days	390	296	294	200	319	213
3 months	488	334	350	225	363	256
6 months	554	385	394	263	413	294

1.4.2. Termkhajornkit, et. al. One ordinary Portland cement mix and three different kinds of fly ash mixes were tested to determine autogenous shrinkage of each mix. Fly ash replacement of 25% and 50% were used for two of the mixes, while the third had only a 50% replacement mix. In order to isolate autogenous shrinkage, the specimens were cast in molds and sealed to avoid evaporation. Strain was measured using a strain gauge placed in the center of the mold with concrete cast around it. The samples were kept in a controlled chamber with constant humidity and temperature. For the two mixes where the fly ash replacement was varied, the higher level (50% replacement) mix showed a significant reduction in measured shrinkage strain. Interestingly, all three mixes with 50% replacement outperformed the conventional mixes, while both 25% replacement mixes underperformed the conventional mixes.

1.4.3. Gao, et. al. RCC concrete typical to dam and pavement construction was tested for shrinkage strain. Shrinkage data was recorded for one baseline mix and one equivalent mix with a 50% cement replacement with fly ash. It was concluded that, at 150 days, the shrinkage strains of the 50% replacement mix was approximately 33% less than that of the specimen without fly ash.

1.4.4. Nath and Sarker. Two different concrete series, labeled as series A and B in this study, were tested for drying shrinkage up to 180 days. Both series had one mix with no fly ash replacement, one mix with 30% replacement, and one mix with 40% replacement. Series A was designed in a way that all three mixes attained similar 28 day compressive strengths. Series B was designed so that all three mixes had an identical water to total binder content ratio (w/b) of 0.29. The results of series A show that, with varying w/b and similar strength, fly ash concretes show less shrinkage as the replacement is increased. Series B shows that with an increase in total cementitious material at a constant w/b, the shrinkage strains shown at 180 days of fly ash mixes are very similar to the control mix. Results are shown in **Figures 1.2 – 1.3**.

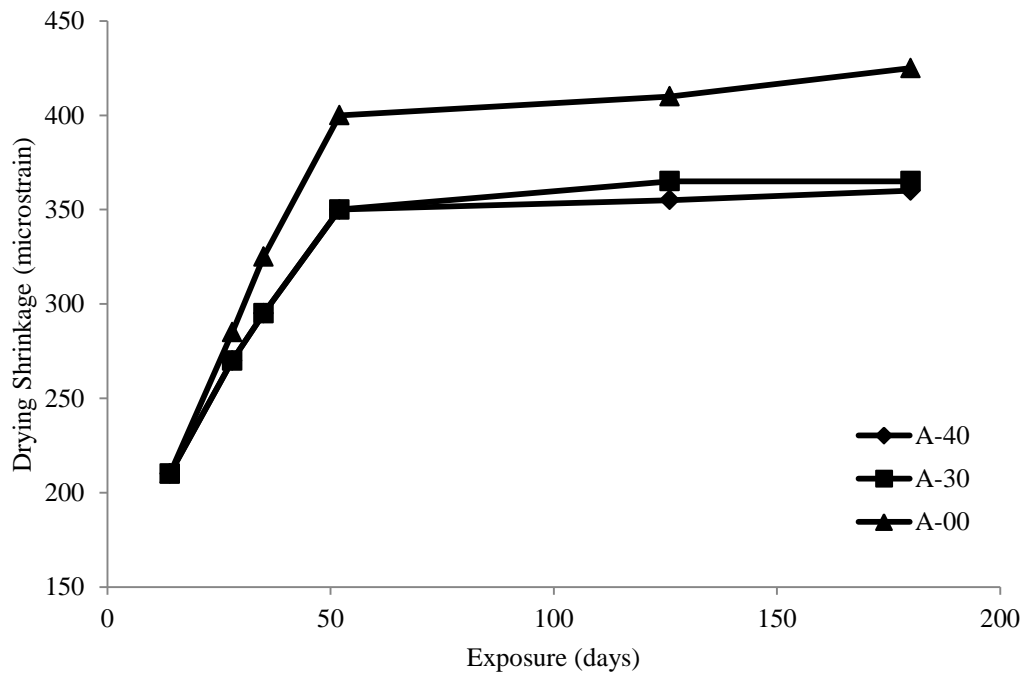


Figure 1.2 - Series A Shrinkage Results (adapted from Nath and Sarker)

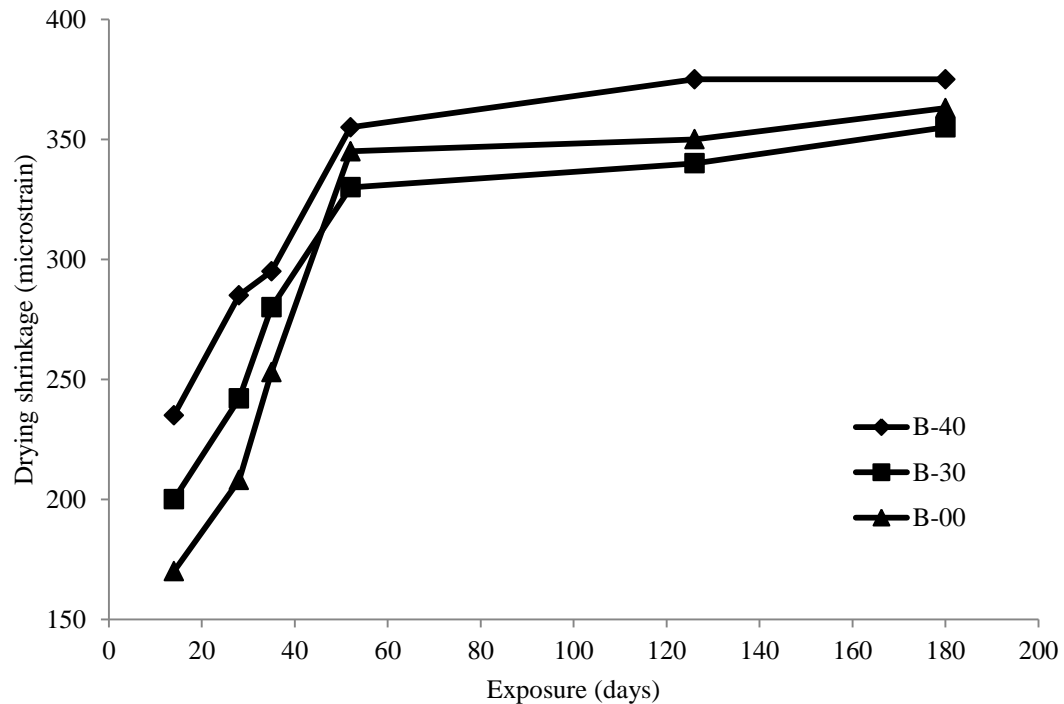


Figure 1.3 - Series B Shrinkage Results (adapted from Nath and Sarker)

1.5. CREEP OF CONCRETE

1.5.1. Definition of Creep. Creep of concrete is defined as “the time-dependent increase in strain under sustained constant load taking place after the initial strain at loading” (ACI 209.1R-05). Initial strain is the short term strain at the moment of loading. Initial strain is difficult to determine as it is very dependent on the duration and rate of initial load and there is no clear distinction between initial strain and creep strain. Creep strain can be broken up into two parts, basic creep and drying creep. Basic creep is “the increase in strain under sustained constant load of a concrete specimen in which moisture losses or gains are prevented.” Even after 30 years of measurement on sealed concrete specimens, it had yet to be determined if basic creep approaches an ultimate value. Drying creep is the additional creep occurring in a specimen exposed to the environment and allowed to dry. The effects of creep can be expressed in three ways. The first is

similar to that of shrinkage, where creep strain is simply expressed in terms of microstrain (strain $\times 10^{-6}$). The second way is called the creep coefficient. The creep coefficient is the ratio of creep strain to the initial strain at loading. The third is specific creep. Specific creep is the ratio of microstrain to applied load (psi).

1.5.2. Factors Affecting Creep. Like shrinkage, creep is affected by numerous material, mix design, environmental, and construction related factors. Similar to shrinkage, the amount, size, gradation, and properties of the aggregate are very influential on creep of concrete. An increase in aggregate volume will decrease creep. Aggregate gradation is believed to influence creep of concrete because of its relation to changes in overall aggregate volume. The size of aggregate affects bond between paste and aggregate, which controls stress concentration and microcracking. Unlike shrinkage, which is primarily affected by properties of the paste, creep is very dependent on the elastic properties of the aggregate. Concretes with aggregate that have a lower modulus of elasticity generally have higher creep. The primary environmental factor in creep is relative humidity. As relative humidity increases, drying creep significantly decreases. Specimens in environments where drying cannot occur may have only one quarter of the creep of concrete which is allowed to dry. The effects of construction and design on creep are slightly different than shrinkage. One similarity is that increased curing time will decrease creep strain. Unlike shrinkage, basic creep is not affected by the size and shape of the member. The factor that most affects creep is the load applied to the specimen. The magnitude of the load, and the age at which the load is first applied are very important. Loads up to $0.40f_c$ are considered to be linearly related to creep. Finally, concrete loaded at later ages has lower creep.

1.6. CREEP MODELS

As with shrinkage, considerable research has been done and models developed to predict the creep potential of concrete. The following sections will present various models for calculating creep.

1.6.1. ACI 209R-92. This model is based on the same research as the ACI 209 shrinkage model. The standard conditions as shown in **Table 1.1** apply to creep as well. **Eq. 1.44 – 1.46** represent the general model for concrete meeting the standard conditions. If standard conditions are met, γ_c is taken to be equal to 1. Like the shrinkage model, if any or all of the standard conditions are not met, the model modification factors must be used as shown in **Eq. 1.47 – 1.53**.

$$\Phi(t, t_0) = \frac{(t-t_0)^\Psi}{d+(t-t_0)^\Psi} \Phi_u \quad (1.44)$$

$$\Phi_u = 2.35\gamma_c \quad (1.45)$$

$$d = 26.0e^{\{0.36(V/S)\}} \quad (1.46)$$

$$\gamma_c = \gamma_{c,to} \gamma_{c,RH} \gamma_{c,vs} \gamma_{c,s} \gamma_{c,\psi} \gamma_{c,\alpha} \quad (1.47)$$

$$\gamma_{c,to} = \begin{cases} 1.25t_0^{-0.118} & \text{for moist curing} \\ 1.13t_0^{-0.094} & \text{for steam curing} \end{cases} \quad (1.48)$$

$$\gamma_{c,RH} = 1.27 - 0.67h \quad (1.49)$$

$$\gamma_{c,vs} = \frac{2}{3}(1 + 1.13e^{\{-0.54(V/S)\}}) \quad (1.50)$$

$$\gamma_{c,s} = 0.82 + 0.067s \quad (1.51)$$

$$\gamma_{c,\psi} = 0.88 + 0.0024\psi \quad (1.52)$$

$$\gamma_{c,\alpha} = 0.46 + 0.09\alpha \geq 1 \quad (1.53)$$

Where: $\Phi(t,t_0)$ is the calculated creep coefficient at a given age, Φ_u is the calculated ultimate creep coefficient, t is the age of the specimen in days, γ_{c,t_0} is the curing condition correction factor, t_0 is the age at which the specimen is loaded in days, $\gamma_{c,RH}$ is the humidity correction factor, h is relative humidity in decimals, $\gamma_{c,VS}$ is the size correction factor, V/S is the volume to surface area ratio, $\gamma_{c,s}$ is the slump correction factor, s is slump in inches, $\gamma_{c,\psi}$ is the fine aggregate correction factor, ψ is the ratio of fine aggregate to total aggregate by weight expressed as percentage, $\gamma_{c,\alpha}$ is the air content correction factor, and α is the air content in percent. For shape and size effects to be totally considered, d is to be determined using **Eq. 1.46** and ψ assumed to be equal to 1.0. Otherwise, average values of $d=10$ and $\psi=0.6$ are to be assumed.

1.6.2. NCHRP Report 496. This proposed creep model was developed in a similar manner to that of the NCHRP Report 496 shrinkage model. The correction factors that are identical to those used in the corresponding shrinkage model have already been defined in Section 1.3.2 The model is shown in **Eq. 1.54 – 1.60**.

$$\psi(t, t_i) = 1.90\gamma_{cr} \quad (1.54)$$

$$\gamma_{cr} = k_{td}k_{la}k_s k_{hc}k_f \quad (1.55)$$

$$k_{td} = \frac{t}{61-4f'_{ci}+t} \quad (1.56)$$

$$k_{la} = t_i^{-0.118} \quad (1.57)$$

$$k_s = \frac{1064-94V/S}{735} \quad (1.58)$$

$$k_{hc} = 1.56 - 0.008H \quad (1.59)$$

$$k_f = \frac{5}{1+f'_{ci}} \quad (1.60)$$

Where: $\psi(t, t_i)$ is the calculated creep coefficient at a given age, k_{td} is the time development factor, t is the age of the concrete in days, k_{la} is the loading factor, t_i is the age at which creep specimen is loaded in days, k_s is the size factor, V/S is the volume to surface area ratio, k_{hc} is the humidity factor, H is the average ambient relative humidity in percent, k_f is the concrete strength factor, and f'_{ci} is the specified compressive strength of concrete in ksi.

1.6.3. CEB-FIP 90. The following equations apply to the creep model as developed jointly by CEB and FIP as presented in the CEB-FIP Model Code 1990.

$$\Phi(t, t_0) = \Phi_0 \beta_c(t - t_0) \quad (1.61)$$

$$\Phi_0 = \Phi_{RH} \beta(f_{cm}) \beta(t_0) \quad (1.62)$$

$$\Phi_{RH} = 1 + \frac{1 - RH}{0.46 \left(\frac{2A_c}{100u} \right)^{1/3}} \quad (1.63)$$

$$\beta(f_{cm}) = \frac{5.3}{(f_{cm}/10)^{0.5}} \quad (1.64)$$

$$\beta(t_0) = \frac{1}{0.1 + t_0^{0.2}} \quad (1.65)$$

$$\beta_c(t - t_0) = \left[\frac{(t - t_0)}{\beta_H + (t - t_0)} \right]^{0.3} \quad (1.66)$$

$$\beta_H = 150 \{ 1 + (1.2RH)^{18} \} \left(\frac{2A_c}{100u} \right) + 250 \leq 1500 \quad (1.67)$$

Where: $\Phi(t, t_0)$ is the calculated creep coefficient at a given age, Φ_0 is the notional creep coefficient, β_c is the coefficient to describe the development of creep with time after loading, t is the age of concrete in days, t_0 is the age of concrete at loading in days, RH is the relative humidity in decimals, A_c is the cross section area in mm^2 , u is the perimeter

in contact with the atmosphere in mm, and f_{cm} is the mean compressive strength of concrete at the age of 28 days in MPa.

1.6.4. GL 2000. As with the GL 2000 shrinkage model, the following creep model was published in the ACI materials journal under the title “Design Provisions for Drying Shrinkage and Creep of Normal-Strength Concrete”.

$$\Phi_{28} = \Phi(t_c) \left[2 \left(\frac{(t-t_c)^{0.3}}{(t-t_c)^{0.3}+14} \right) + \left(\frac{7}{t_0} \right)^{0.5} \left(\frac{t-t_c}{t-t_c+7} \right)^{0.5} + 2.5(1 - 1.086h^2) \left(\frac{t-t_0}{t-t_0+97(V/S)^2} \right)^{0.5} \right] \quad (1.68)$$

$$\Phi(t_c) = \left[1 - \left(\frac{t-t_c}{t-t_c+97(V/S)^2} \right)^{0.5} \right]^{0.5} \quad (1.69)$$

Where: Φ_{28} is the calculated creep coefficient at a given age, $\Phi(t_c)$ is a factor that takes into account drying before loading, t is age of concrete in days, t_c is the age of concrete when drying begins, t_0 is the age the concrete was loaded, h is humidity in decimals, and V/S is the volume to surface area ratio in mm.

1.7. HVFA CREEP RESEARCH

Research has shown that the replacement of Portland cement with fly ash produces concrete which exhibits lower long term creep. Suggested reasons why this is true are discussed in the following sections.

1.7.1. ACI 232.2R-03. The ACI 232.2R committee report cites several sources that have researched creep of fly ash concrete. Lane and Best showed that, when formulated to have the same compressive strength at the age of testing, fly ash concretes

display lower shrinkage. It is suggested that this is due to the higher late age strength of fly ash concrete.

1.7.2. Alexander, et. al. Concrete with 25% fly ash replacement was tested for creep up to the age of 6 years. The specimens were tested at loads of 25% and 40% of 28 day compressive strength. A control conventional concrete mix was also tested simultaneously. All specimens tested had a strength of 4000 psi (27.58 MPa) at 28 days. The results show that concrete without fly ash showed 50% higher creep than concrete which had 25% fly ash replacement. These results were recorded at two years of age, and remained unchanged up to six years.

1.8. APPLICATION OF SHRINKAGE AND CREEP

1.8.1. Prestress Loss. Prestress loss is “the loss of compressive force acting on the concrete component of a prestressed concrete section” (NCHRP 426). The ability to accurately predict the prestress loss in beams is very dependent on the ability to predict the beam’s shortening due to shrinkage and creep. Shortening of the beam reduces the tensile force in the prestressed reinforcement and must be accounted for in design. NCHRP 426 names three components which significantly affect the prestress loss in pretensioned concrete members which directly relate to shrinkage and creep. These components are:

1. Instantaneous prestress loss due to elastic shortening at transfer of force from prestressed reinforcement to concrete.
2. Long-term prestress loss due to shrinkage and creep of concrete and relaxation of prestressing strands between the time of transfer and deck placement.

3. Long-term prestress loss between the time of deck placement to the final service life of the structure due to shrinkage and creep of the girder.

Figure 1.4 shows the prestress loss over the life cycle of a pretensioned concrete girder. The loss between points D and E represent the loss due to creep, shrinkage, and relaxation of prestressing strands.

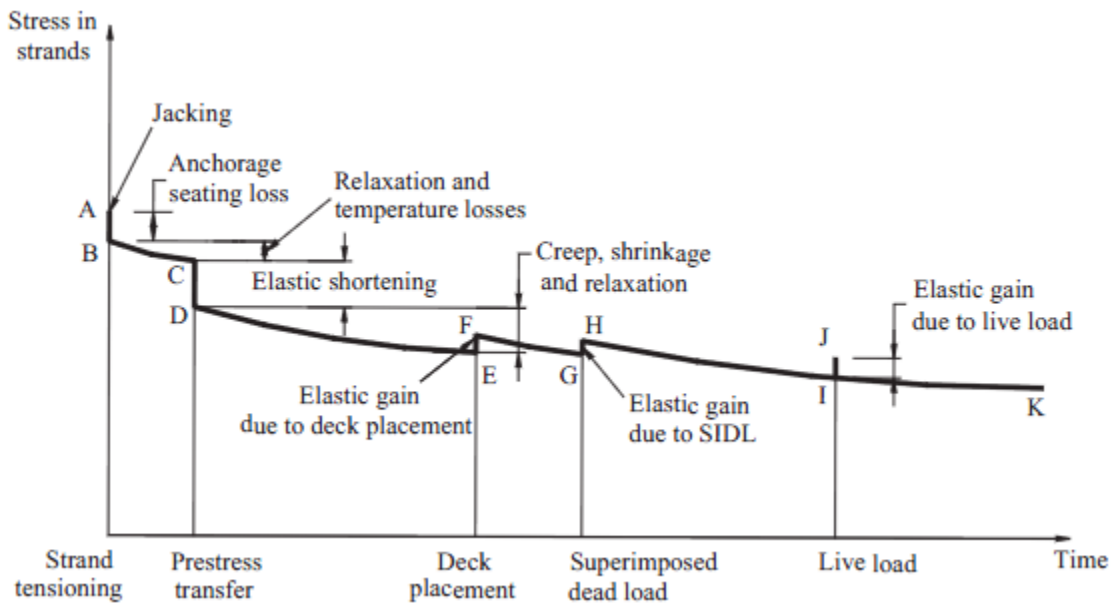


Figure 1.4 - Stress vs. Time for Prestressed Bridge Girder (Tadros et. al. 2003)

1.8.2. Load Effects. The procedures in “Design of Continuous Highway Bridges with Precast, Prestressed Concrete Girders” published by the Portland Cement Association (PCA) take into account additional moments due to shrinkage and creep when determining loads for design. In this method, fixed end moments due to creep and end driving moments due to shrinkage are calculated. These applied moments result from a continuity connection being made at supports by the placement of the bridge deck. The placement restricts free rotation of the beams and therefore produces moment in the

connection. The moments calculated by this method are then added to all other load effects at all sections for determination of the ultimate design load. The shrinkage driving moment calculation is done by first calculating theoretical ultimate shrinkage values for the beam and the slab. The differential shrinkage between the beam and slab are then used to determine an applied moment due to shrinkage. The applied moment due to creep results from prestressed creep and dead load creep. Theoretical creep coefficients are calculated for the time before and after deck placement. The creep that occurs after deck placement is what contributes to the applied moment.

1.8.3. Beam Deflection. Shrinkage and creep must also be accounted for when calculating long term deflection of flexural members. Eq. 9-11 of ACI 318-08, shown here as **Eq. 1.70**, accounts for long term sustained loads. This factor is multiplied by the immediate deflection caused by the load considered.

$$\lambda_{\Delta} = \frac{\xi}{1+50\rho'} \quad (1.70)$$

Where: λ_{Δ} is the multiplier for additional deflection due to long-term effects, ξ is the time dependent factor for sustained load, and ρ' is compression reinforcement ratio.

1.9. CONCRETE ABRASION

1.9.1. Definition of Concrete Abrasion. Abrasion is the physical wearing down of a material. The most common sources of abrasion of concrete structures are by the friction between vehicle tires and concrete pavement road surfaces, and by water

flows over exposed dam or bridge footings. Concrete abrasion leads to a decrease in member thickness which can lead to cracking or failure of the structure (Atis).

1.9.2. Factors Affecting Concrete Abrasion. Several material properties and construction factors can affect the abrasion resistance of concrete. The concrete strength is the most influential property in regards to abrasion resistance. The properties of the aggregate are also very important in a concrete's resistance to abrasion. The surface finish and whether or not a hardener or topping is used effects abrasion resistance as well (Naik et. al.).

1.10. HVFA ABRASION RESEARCH

There is considerable data available on the abrasion resistance of HVFA concrete. The motivation for research of HVFA concrete abrasion resistance is that HVFA concrete has been proposed as a possible material for paving.

1.10.1. Naik, et. al. The objective of this testing program was to determine the abrasion resistance of HVFA concrete mixes. Three sources of fly ash were used. Mixes containing 40%, 50%, and 60% fly ash were tested according to a modified version of ASTM C944 for each source along with one convention concrete mix. In this study, depth of wear was used as the measure of value. Results show that above 50%, abrasion resistance of fly ash mixes is slightly lower than that of the reference mix. Results also show that, above all, the concrete's strength was the most influential factor in abrasion resistance.

1.10.2. Atis. The objective of this program was to determine the abrasion resistance of HVFA concrete for use as a pavement material. Five different mixes were tested. One baseline mix, two 50% HVFA mixes, and two 70% HVFA mixes were tested in accordance to BSI 1993 – British Standards Institute “Method for determination of aggregate abrasion value (AAV).” This test method is similar to ASTM C944, which was followed during testing of specimens in this report. Mass loss was the measure of value in this test. Again, results show that abrasion resistance is primarily dependent on the concrete’s strength rather than fly ash content. However results also suggest that at higher strengths, the 70% fly ash mix showed higher resistance than the 50% mix and conventional mix, but at lower strengths the opposite is true.

2. RESEARCH PROGRAM

2.1. MIX DESIGNS

2.1.1. HVFA. The HVFA concrete testing program consisted of three mixes. The first mix tested was a conventional concrete baseline mix (HVFA-C), based on a MoDOT standard mix design. The other two were HVFA concrete mixes. Both HVFA concrete mixes had 70% Class C fly ash replacement, one with a relatively high amount of total cementitious material (HVFA-H) and the other with a relatively low amount of total cementitious material (HVFA-L). The HVFA-H mix design was based on research done by Ortega (2010) at Missouri S&T. The HVFA-L mix design was a modification of the control baseline mix. Both HVFA concrete mixes were batched with the assistance of a local ready mix concrete supplier (Rolla Ready Mix). A partial mix was delivered, with the gypsum, calcium hydroxide, and HRWR added upon arrival. The mix designs tested can be found in **Table 2.1** along with the measured 28 day compressive strength (f'_c) and modulus of elasticity (MOE). All aggregate weights found in **Table 2.1** are based on SSD conditions.

Table 2.1 - HVFA Test Program Mix Designs and mechanical properties

Material	Amount (per cubic yard)		
	HVFA-C	HVFA-H	HVFA-L
Water	226 lb.	321 lb.	226 lb.
Cement (Type I)	564 lb.	219 lb.	155 lb.
Coarse Aggregate (3/4" JC Dolomite)	1860 lb.	1754 lb.	1754 lb.
Fine Aggregate (Missouri River Sand)	1240 lb.	1080 lb.	1080 lb.
Fly Ash	N/A	511 lb.	360 lb.
Gypsum	N/A	20.4 lb	14.4 lb.
Calcium Hydroxide	N/A	51.1 lb.	36 lb.
BASF Glenium 7500 (HRWR)	3.0 fl oz/cwt	N/A	3.0 fl oz/cwt
f'c (psi)	5,400	3,100	3,500
MOE (psi)	3,386,000	3,475,000	3,163,000

Conversion: $1 \text{ kg/m}^3 = 1.686 \text{ lb/yd}^3$

1 fl oz = 26.57 mL

1 psi = 6.89 kPa

2.2. SHRINKAGE AND CREEP SPECIMEN CONSTRUCTION

2.2.1. Shrinkage and Creep Specimens. Both shrinkage and creep testing were done using identical specimens. Although only four specimens per mix were necessary for testing (two each for shrinkage and creep), six specimens per mix were cast in case any specimens were damaged during de-molding. These specimens were fabricated and prepared as described below.

2.2.2. Shrinkage and Creep Molds. The molds for the shrinkage and creep specimens were 4 in. diameter PVC pipe adhered to a plywood base. The PVC was cut into 24 in. sections with care being taken to ensure all cuts were made so that the mold would sit flush and orthogonal to the base. The PVC was also notched on opposite sides. The notches made de-molding much easier and significantly reduced the possibility of damaging the specimens during de-molding. Once prepared the PVC was adhered to a 1

ft. (304.8 mm) by 1 ft. (304.8 mm) plywood base using a waterproof silicon sealant. The completed molds were allowed to sit for at least 24 hours before use to allow for the sealant to fully set up. **Figure 2.1** shows a completed shrinkage and creep mold.



Figure 2.1 - Shrinkage and Creep Form

2.2.3. Shrinkage and Creep Specimen Casting. Specimens were consolidated in a manner similar to that prescribed in ASTM C31 “Standard Practice for Making and Curing Concrete Test Specimens in the Field” for a 6 in. diameter cylinder. Consolidation and vibration were performed when necessary. The specimens were cast in three layers of approximately equal depth and were rodded 25 times per layer. External vibration was

also performed after each layer was rodded using an electric handheld concrete vibrator as needed. Specimens were moist cured until de-molded and prepared.

2.2.4. Shrinkage and Creep De-Molding and Preparation. All specimens were de-molded within 24 hours of their initial set time. De-molding was done by first cutting through the notched section with a utility knife. A hammer and chisel were then used to split the mold and remove it from the concrete. Creep specimens were sulfur capped on both ends in preparation for loading at 28 days. Shrinkage specimens were sulfur capped on only the bottom end, allowing for stability and more accurate readings.

2.2.5. Shrinkage and Creep Data Acquisition. A demountable mechanical strain gauge (DEMEC) was used to measure strain in the concrete. DEMEC points, small pre-drilled stainless steel discs, were adhered to the surface of the specimen. They were arranged in three vertical lines of five points, 120° apart, as shown in **Fig. 2.2**. This arrangement allowed for 9 readings to be taken per specimen. The average of all readings taken per specimen was taken as the value to be used for strain calculation. The points in one line per specimen were adhered using gel control super glue. The instant hardening allowed for initial readings to be made on each specimen as soon as possible. The remaining points were adhered using concrete/metal epoxy, which took up to 24 hours to fully harden for accurate reading to be taken. The points adhered with super glue were later protected using the epoxy.

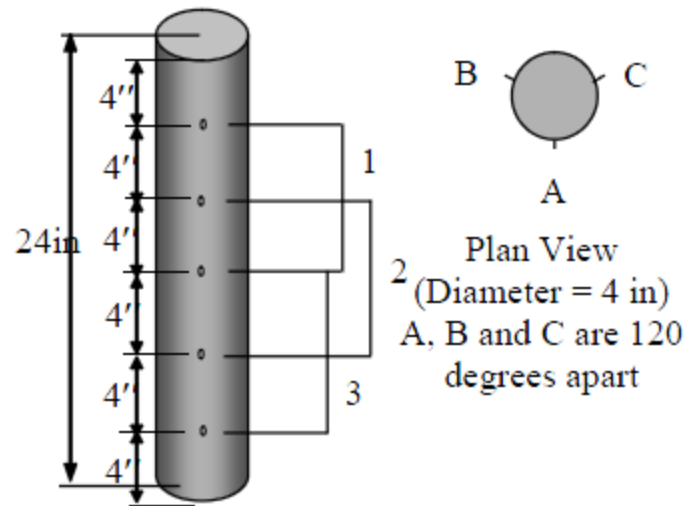


Figure 2.2 – Shrinkage and Creep Specimens and DEMEC Point Arrangement (Myers and Yang, 2005)

2.3. ABRASION SPECIMEN CONSTRUCTION

One specimen per mix was cast for abrasion test. Each specimen was large enough so that three replicate abrasion tests could be done for each mix. Abrasion specimens measured 6 in. (152.4 mm) by 16 in. (406.4 mm) by 3.5 in. (88.9 mm) and were cast in a mold made from wooden 2x4 sections and attached to a plywood base. The baseline and HVFA concrete mixes were consolidated similar to that prescribed in ASTM C31 “Standard Practice for Making and Curing Concrete Test Specimens in the Field” for a 6 in. (152.4 mm) wide beam. External vibration was used as necessary. To ensure that abrasion tests on all specimens were consistent, every specimen tested was finished by the same individual using a hand trowel. Specimens were moist cured until tested. All testing was performed on the top finished surface of the specimen.

2.4. TESTING PROCEDURES

2.4.1. Shrinkage Testing Procedures. A modified version of ASTM C157 “Standard Test Method for Length Change of Hardened Hydraulic-Cement Mortar and Concrete” was used to determine the shrinkage of the concrete specimens. Until the age of loading for creep, four specimens were used for shrinkage determination. At 28 days, two of these specimens were transferred to creep frames, leaving two remaining specimens to be tested for long term shrinkage. Nine strain readings could be taken per specimen, with the average of all readings taken as the value to be used for shrinkage calculation. Strain was determined using the DEMEC readings and calculated by **Eq. 2.1** as found in “Simplified Instructions for Using a Digital DEMEC Gauge”. An example of a DEMEC reading being taken on a specimen is in **Figure 2.1**. Readings were normalized by taking a reading on the reference bar, shown in **Figure 2.2** with a reading taken on the reference bar shown in **Figure 2.3**. Shrinkage strain experienced during the first day after demolding was estimated based on linear interpolation of subsequent strain values, as calculated by **Eq. 2.1**

$$\Delta\varepsilon_s = G((R_i - R_0) - (D_i - D_0)) \quad (\mu\varepsilon) \quad (2.1)$$

Where: $\Delta\varepsilon_s$ is the change in strain from one reading to the next, G is the gauge factor shown in **Figure 2.3**, 0.400×10^{-5} strain per division (4 microstrain), D_0 is the datum reading on the reference bar, D_i is the subsequent reading on the reference bar, R_0 is the datum reading on the tested material, and R_i is the subsequent reading on the tested

material. Gauge units are the digital gauge reading without the decimal point. For example, **Figure 2.4** shows a reading of 2.523 which equates to 2523 gauge units.



Figure 2.3 – DEMEC Reading Taken on Specimen



Figure 2.4 - Reference Bar



Figure 2.5 - Reading Taken on Reference Bar



Figure 2.6 - Gauge Factor Used for Shrinkage and Creep Calculations



Figure 2.7 - Example DEMEC Gauge Reading

2.4.2. Creep Testing Procedures. A modified version of ASTM C512 “Standard Test Method for Creep of Concrete in Compression” was used to determine the creep of the concrete specimens tested. Until the age of loading, creep specimens acted as shrinkage specimens. This is a modification of ASTM C512, as the specimens were not moist cured beyond the time of de-molding. Additionally, humidity was not controlled however it was recorded.

At 28 days, representative specimens were tested according to ASTM C39 “Standard Test Method for Compressive Strength of Cylindrical Concrete Specimens” and ASTM C469 “Standard Test Method for Static Modulus of Elasticity and Poisson’s Ratio of Concrete in Compression.” Creep specimens were then loaded to 40% of their measured 28 day compressive strength in the creep frames shown in **Figures 2.8 – 2.9**. The design of the creep frames was based on research done by Myers and Yang (2005).

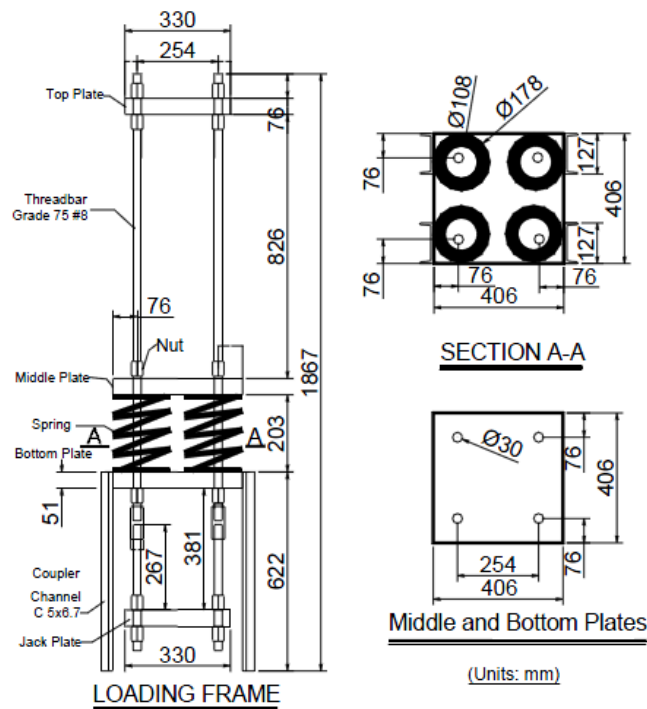


Figure 2.8 - Schematic of Creep Loading Frame (Myers and Yang, 2005)
(1 in = 25.4 mm)



Figure 2.9 - Creep Loading Frame with Specimen

Measurements taken on creep specimens were done in the exact way as with the shrinkage specimens. **Eq. 2.2** was used to determine the change in strain between one creep reading to the next. Using the calculated creep strain, the coefficient of creep could be determined by **Eq. 2.3**. Creep and shrinkage readings for like specimens were taken at the same interval. Readings were also taken immediately before and after loading to determine initial elastic strain due to loading. **Figure 2.10** shows a reading being taken on a creep specimen.

$$\Delta\varepsilon_c = G((R_i - R_0) - (D_i - D_0)) - \Delta\varepsilon_s \text{ (}\mu\varepsilon\text{)} \quad (2.2)$$

Where: $\Delta\varepsilon_c$ is the change in creep strain between readings.

$$\Phi(t, t_0) = \varepsilon_t / \varepsilon_i \quad (2.3)$$

Where: $\Phi(t, t_0)$ is the measured creep coefficient at a given age, ε_i is the measured strain due to initial loading of the specimen, ε_t is the measured creep strain at a given age.



Figure 2.10 - Reading Taken on Creep Specimen

2.4.3. Abrasion Resistance Testing Procedures. ASTM C944 “Standard Test Method for Abrasion Resistance of Concrete or Mortar Surfaces by the Rotating-Cutter Method” was used to determine abrasion resistance. A schematic of the rotating cutter used is shown in **Figure 2.11**, which is taken from ASTM C944. The actual rotating cutter is shown in **Figure 2.12**. Abrasion specimens were moist cured until testing at 28 days age. The two HVFA concrete mixes were also tested after an additional 10 weeks of moist cure to further investigate how the late age strength gain of HVFA concrete affected abrasion resistance. One specimen per mix was constructed, which allowed for three abrasion tests. One abrasion test consisted of three abrasion cycles. Each cycle lasted two minutes. A load of 44lb, defined as a double load in ASTM C944, was applied at a rate of 300 rpm using a drill press as shown in **Figure 2.13**. After each cycle, mass loss (mg) was recorded by subtracting the final weight from the initial weight. Each cycle per test was done on the same spot. After completion of each abrasion test, the average depth of wear (mm) was measured using digital calipers. The average depth of wear was calculated from a total of eight depth measurements relative to the adjacent untested surface, four taken on the outer perimeter of the tested surface and four taken around the inner perimeter, at the points indicated in **Figure 2.14**. The measurements were made using a digital caliper. On the day of testing, the specimen was removed from moist cure and surface dried by blotting with paper towels. This was done to avoid any mass loss due to moisture loss. A completed specimen after all three abrasion tests is shown in **Figure 2.15**.

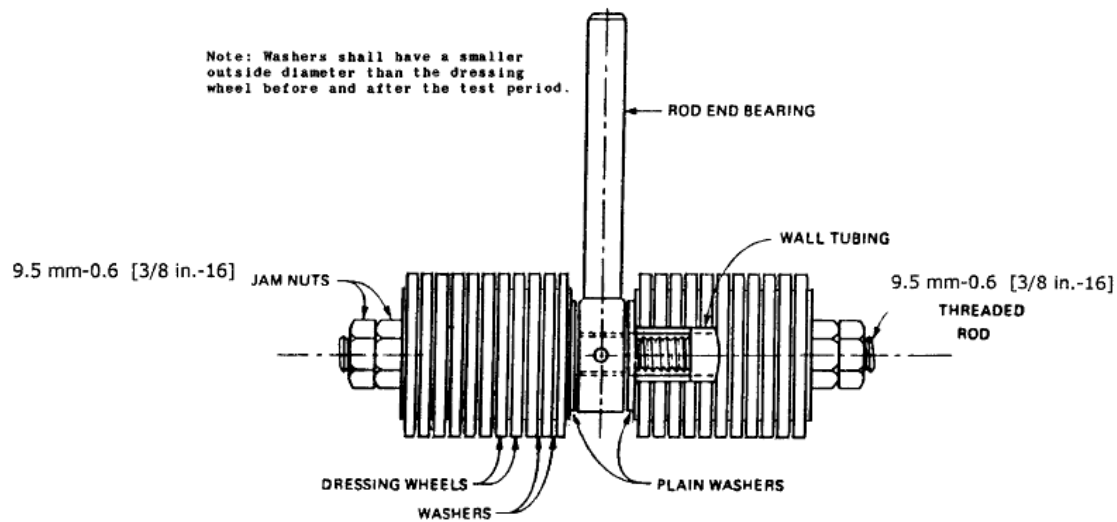


Figure 2.11 - Schematic of Abrasion Rotating Cutter (ASTM C944)
(1 in = 25.4 mm)



Figure 2.12 - Rotating Cutter



Figure 2.13 - Abrasion Resistance Test in Progress



Figure 2.14 - Depth of Wear Measurement Points

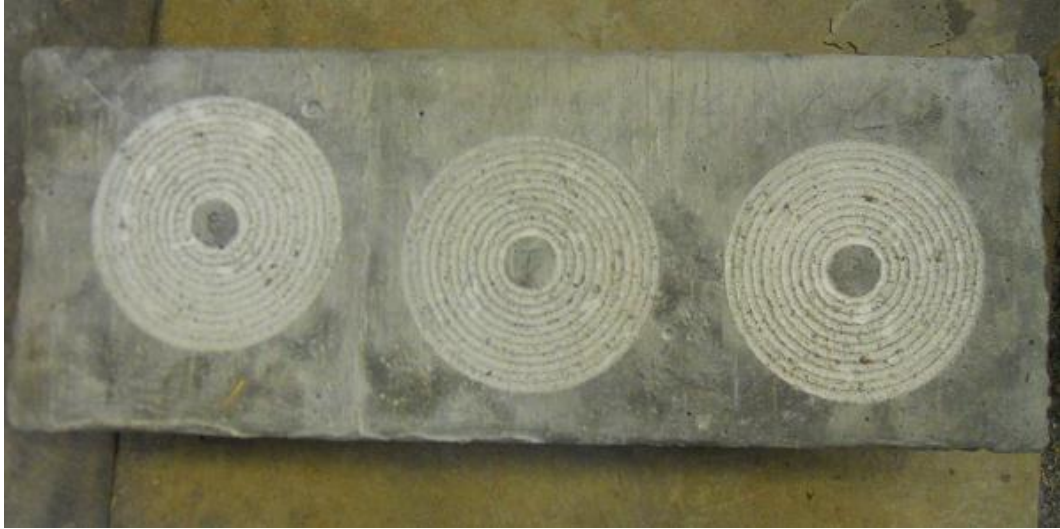


Figure 2.15 - Abrasion Resistance Specimen after Testing

3. HVFA RESULTS AND DISCUSSION

3.1. SHRINKAGE

3.1.1. Results. Figures 3.1 – 3.3 show the experimental data obtained from shrinkage tests of the HVFA concrete plotted with the various prediction models discussed in Section 1. Figure 3.4 shows the experimental results of all four mixes plotted with one another. In figures where different data sources are together, the source of the data can be found in parentheses after the data label in the legend of its respective figure. For all specimens tested for this study, the notation (S&T) will be used.

3.1.2. Conclusions and Discussion. For both HVFA concrete mixes, results were very consistent with data from numerous previous research projects described in sections 1.4.1-1.4.4. It was expected that the two HVFA concrete mixes would experience a decrease in shrinkage strain relative to the conventional mix. It was also expected that HVFA-L, due to the lower level of cementitious material, would experience a further decrease in shrinkage strains.

Both HVFA-H and HVFA-L showed a significant decrease in shrinkage strain relative to HVFA-C. Therefore, for use in practice when shrinkage is a design concern, both HVFA mixes are superior to their equivalent conventional concrete mix.

When comparing results to previous studies, both HVFA-H and HVFA-L performed as expected. Figures 3.5 – 3.6 show the results of HVFA-H and HVFA-L plotted against shrinkage results from Marlay (2011) and Atis (2003) both of which tested HVFA concrete specimens with 70% replacement of Portland cement with fly ash, in addition to two mixes with 50% replacement for comparison. The results from Marlay and Atis validate the relatively low shrinkage strains experienced by HVFA-H and

HVFA-L compared to conventional concrete. Both databases together with experimental results are shown in **Figure 3.7**.

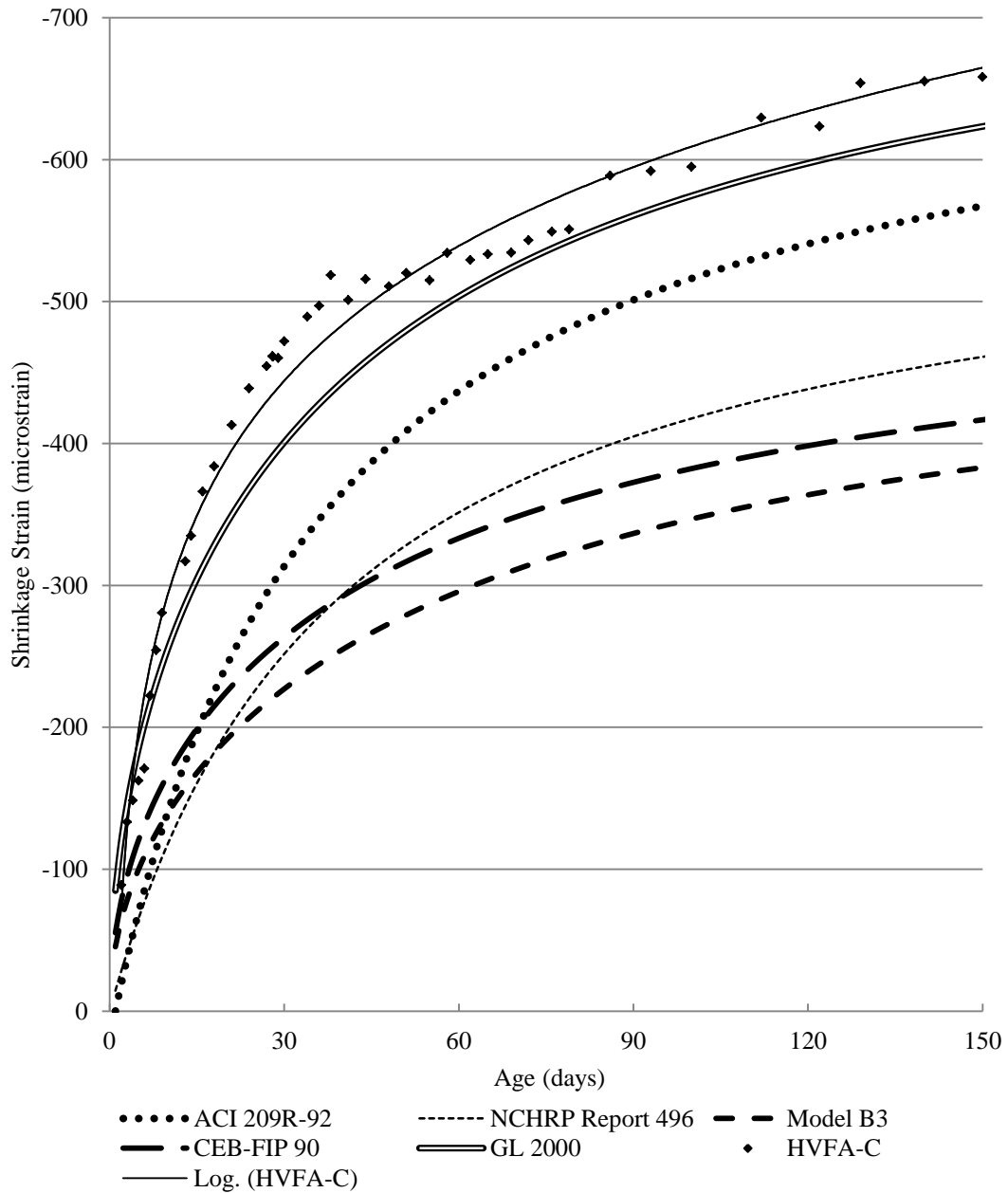


Figure 3.1 - HVFA-C Shrinkage Results and Prediction Models

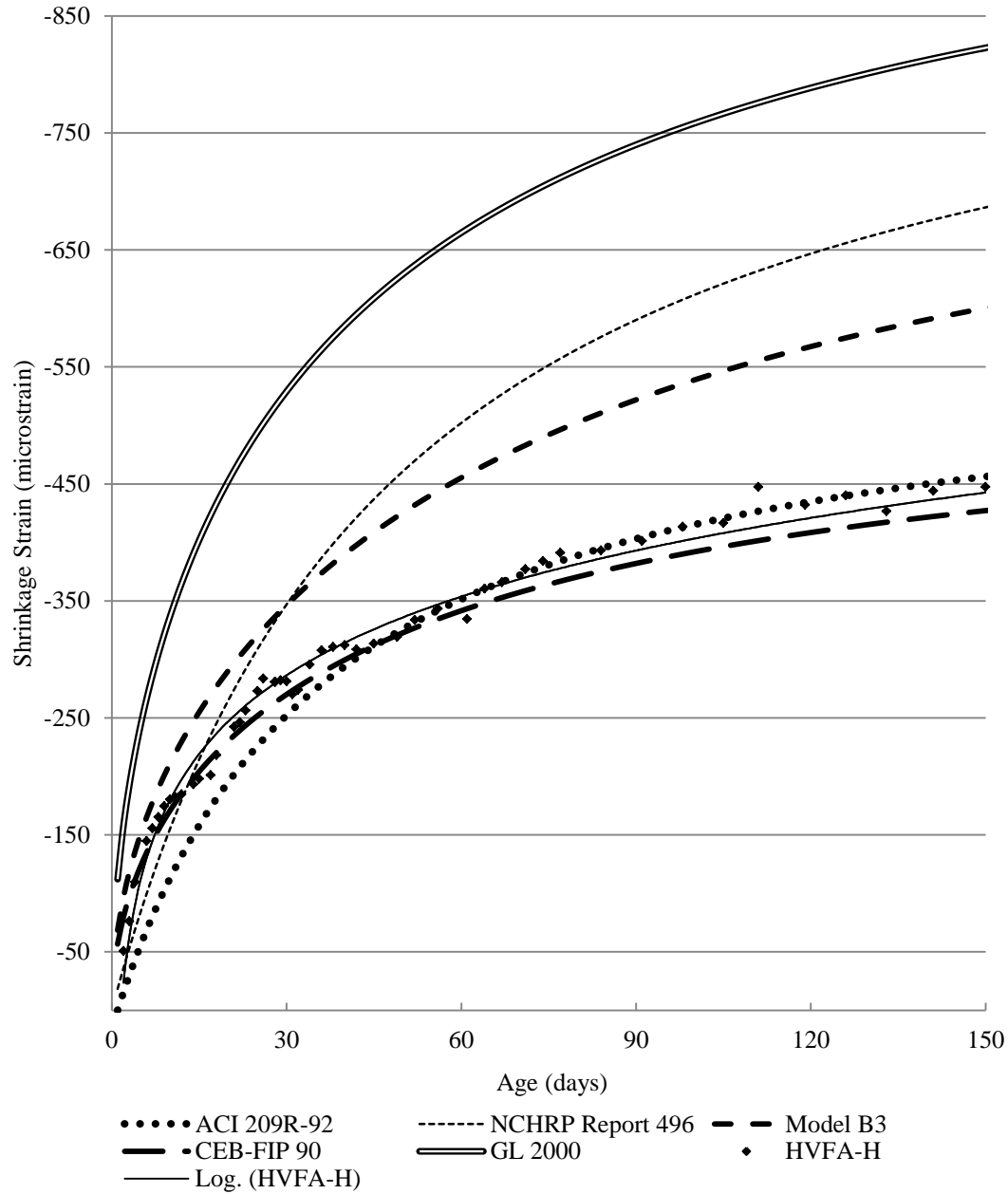


Figure 3.2 - HVFA-H Shrinkage Results and Prediction Models

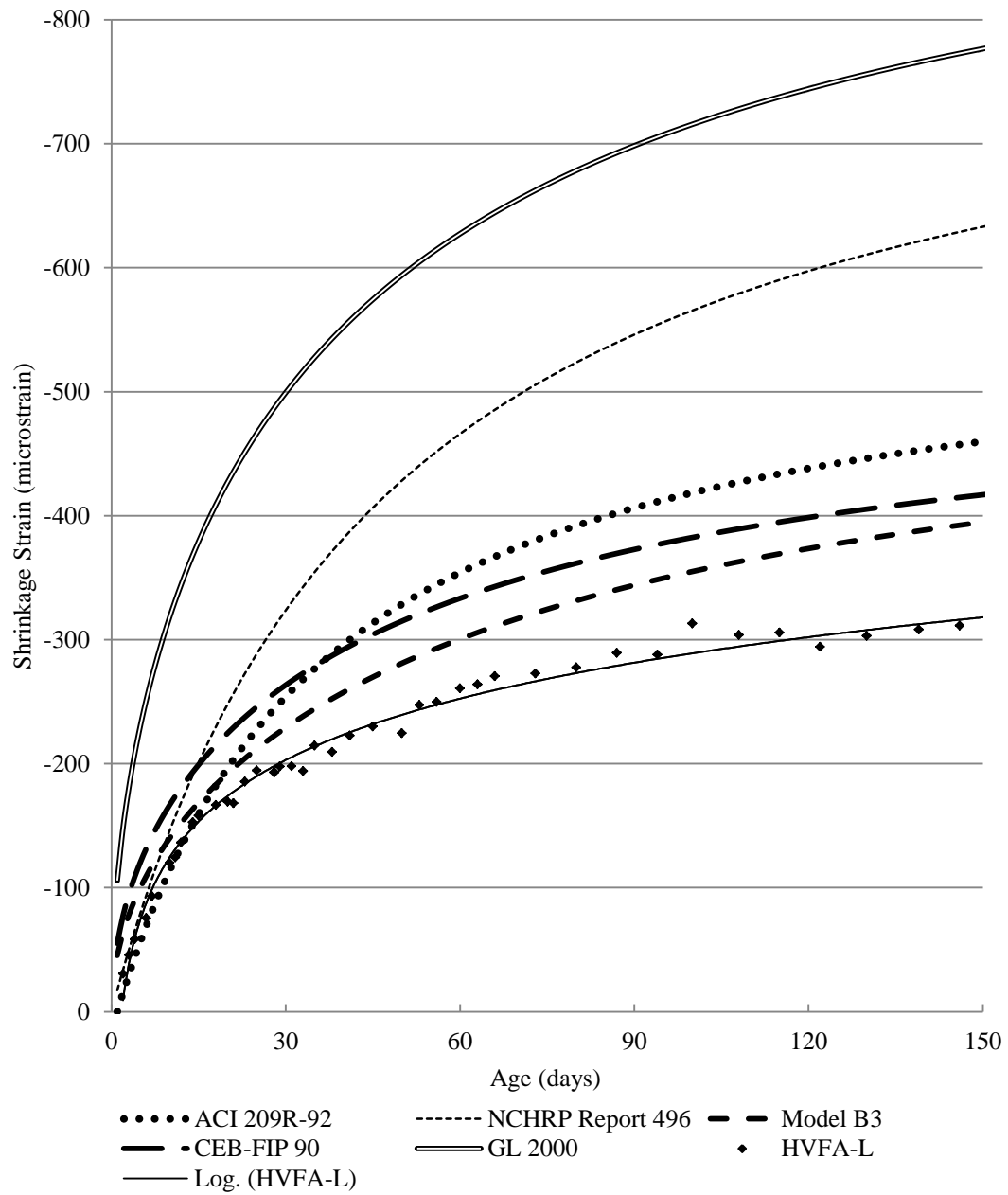


Figure 3.3 - HVFA-L Shrinkage Results and Prediction Models

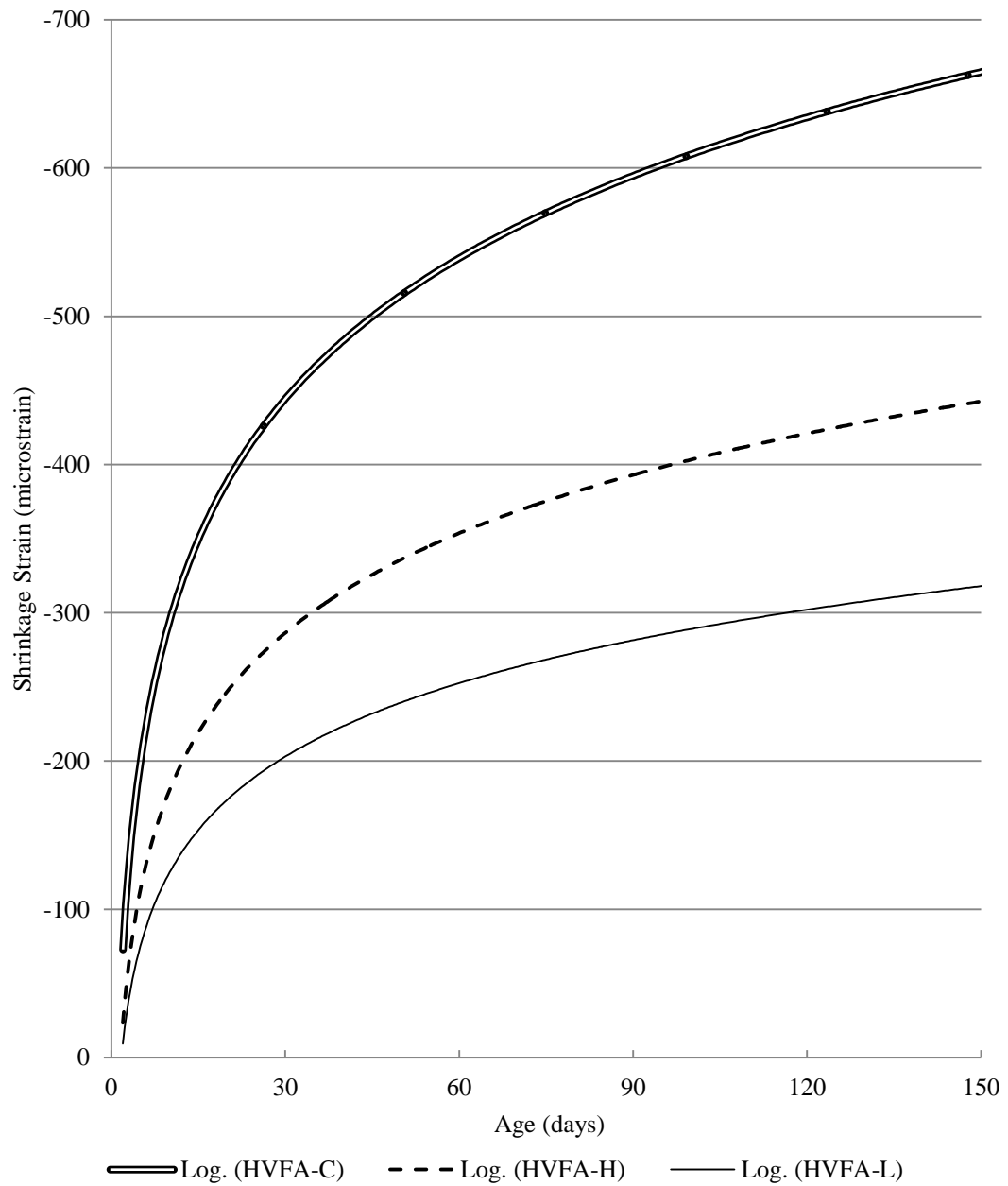


Figure 3.4 – HVFA Shrinkage Results (Best fit Logarithmic)

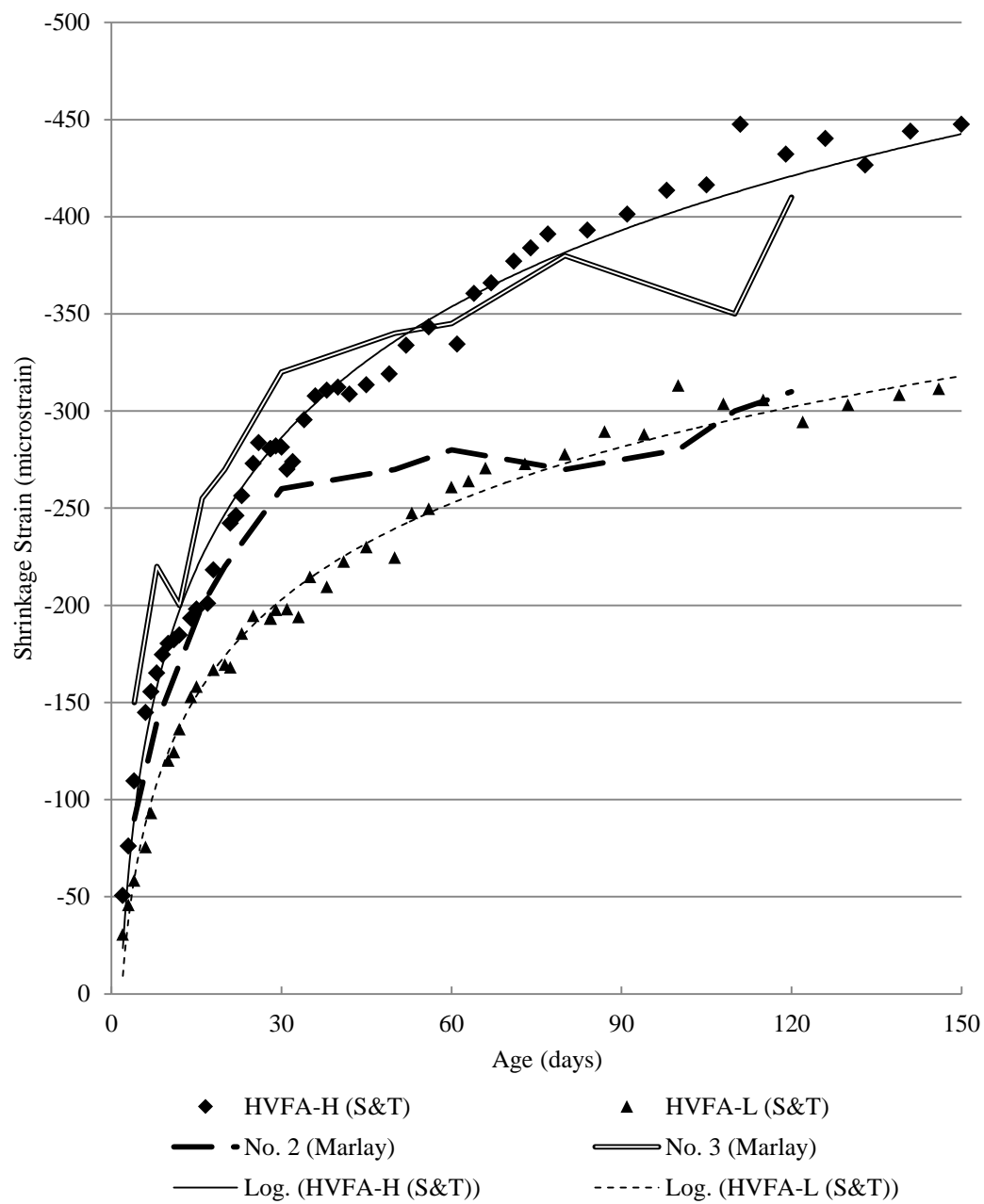


Figure 3.5 – HVFA Shrinkage Results Compared to Marlay (2011)

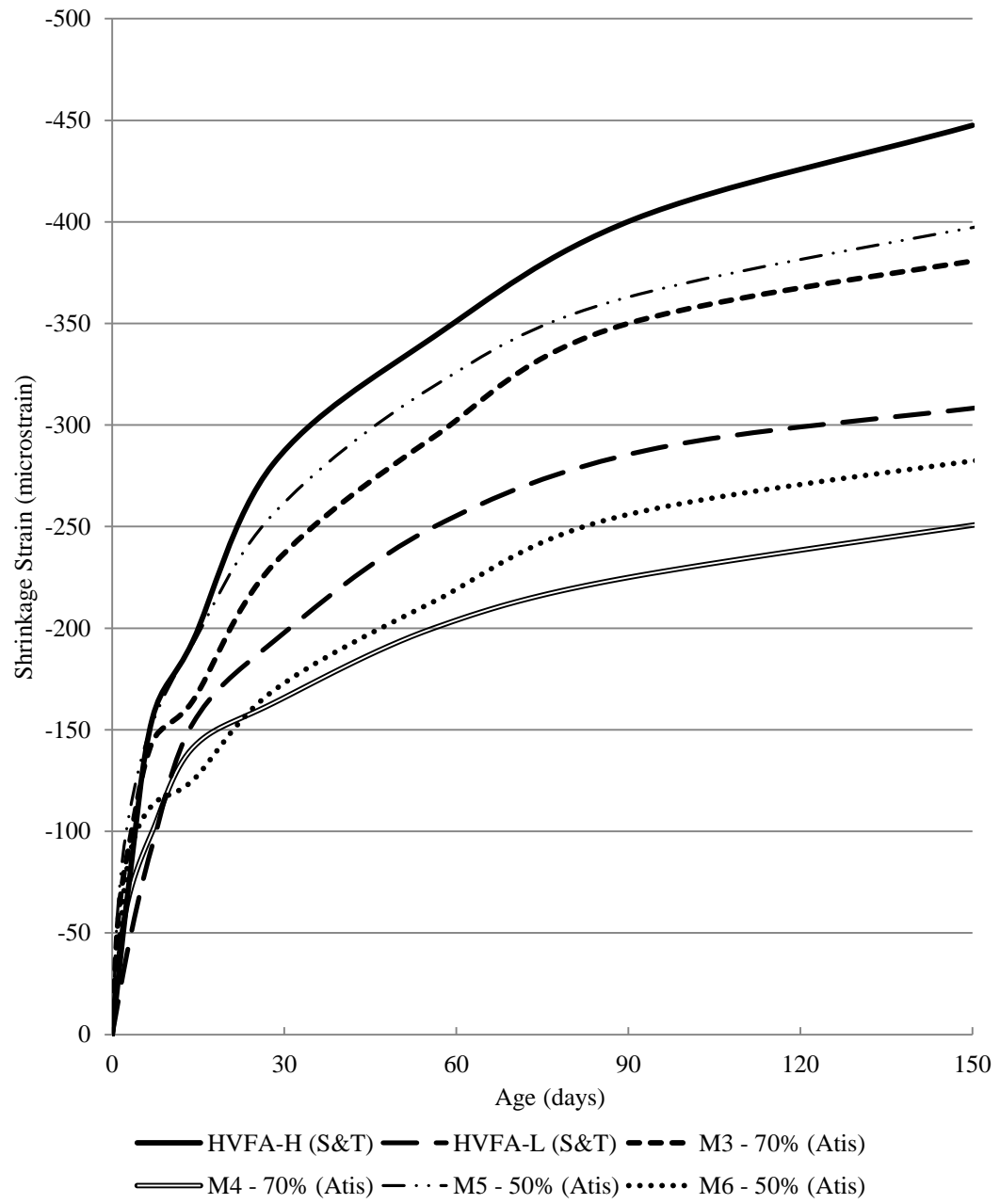


Figure 3.6 – HVFA Shrinkage Results Compared to Atis (2003)

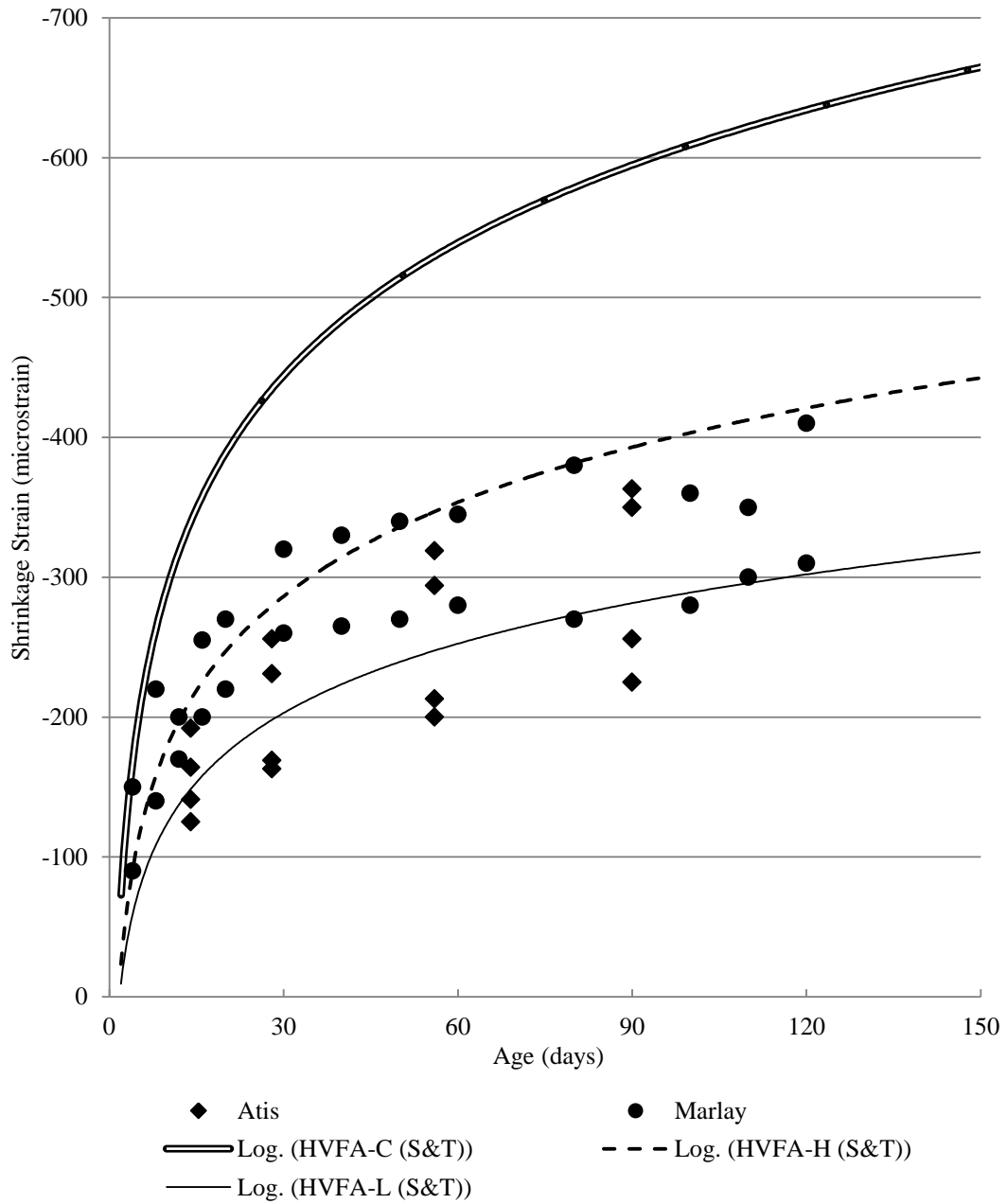


Figure 3.7 – HVFA Results with Shrinkage Databases

3.2. CREEP

3.2.1. Results. Creep Results are shown in **Table 3.1.**

Table 3.1 - Summary of HVFA Creep Results

Creep Strain (microstrain)				
Specimen	Days After Loading			
	7	14	56	126
HVFA-C	296	397	707	1070
HVFA-H	256	333	596	791
HVFA-L	178	225	377	489
Percentage of 126 Day Creep				
HVFA-C	28	37	66	100
HVFA-H	32	42	75	100
HVFA-L	36	46	77	100
Measured Creep Coefficient				
HVFA-C	0.464	0.622	1.12	1.68
HVFA-H	0.463	0.603	1.08	1.43
HVFA-L	0.421	0.533	0.893	1.16
Specific Creep ($\mu\epsilon/\text{psi}$)				
HVFA-C	0.137	0.184	0.327	0.496
HVFA-H	0.206	0.269	0.481	0.638
HVFA-L	0.128	0.162	0.271	0.351

Conversion: 1 MPa = 145.04 psi

3.2.2. Discussion and Conclusions. With the exception of HVFA-H in terms of specific creep, both HVFA concrete specimens outperformed the conventional concrete specimens in creep testing. Both HVFA concrete specimens experienced significantly less creep strain at 126 days after loading than the conventional concrete mix. Creep strain data may be misleading due to the fact that HVFA specimens were loaded at lower levels than conventional concrete due to their decreased compressive strengths at the time of loading. To normalize results, specific creep can be examined. As mentioned above, HVFA-H performed poorly in creep when taken in terms of specific creep. As the specimens got older, however, specific creep of HVFA-H got closer to that of HVFA-C.

At early ages, all three mixes tested showed similar behavior under load, however as the specimens got older, the advantage of HVFA concrete over conventional concrete became more clear. This is demonstrated best by the percentage of 126 day creep. The data shows that during the first two weeks of loading, the HVFA concrete specimens experienced a greater percentage of their ultimate creep strain than did the conventional concrete specimens. However, due to the tendency of HVFA concrete to gain strength at later ages, creep performance improved as the specimens got older.

This late age improvement in creep behavior is exactly what was discovered by Lane and Best, as summarized in ACI 232.2R-03. It was determined that since HVFA concrete had a lower strength at time of loading with increase in strength gain as it aged, its creep behavior would be superior to that of conventional concrete. Additionally, it was shown that concrete with fly ash which had the same strength as conventional concrete still produced less creep at all ages. These properties of creep of HVFA concrete were again confirmed by the results gained in this study.

3.3. ABRASION RESISTANCE

The following sections contain all measured data resulting from abrasion resistance testing along with discussions and conclusions.

3.3.1. Results. **Figures 3.8 – 3.10** show the mass losses recorded after each abrasion cycle for each mix tested. **Figures 3.11 – 3.12** show the relative abrasion resistance of each HVFA concrete specimen by age. **Figures 3.13 -3.14** show the results of all specimens tested together. **Table 3.2** shows a summary of all results along with measured 28 day compressive strength.

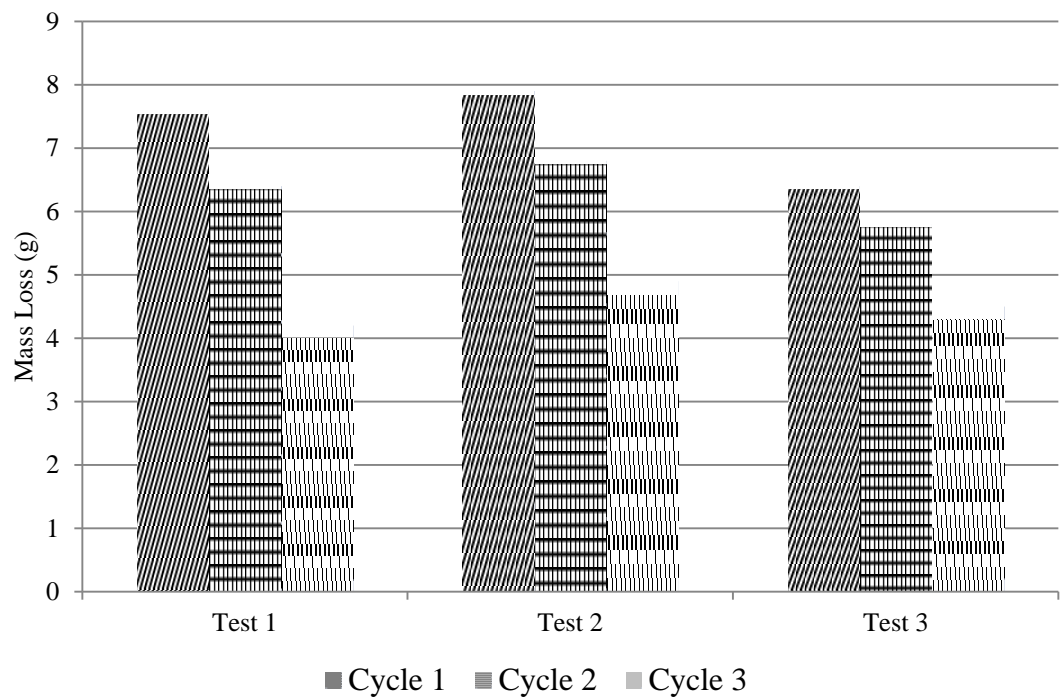


Figure 3.8 - HVFA-C Mass Loss Results

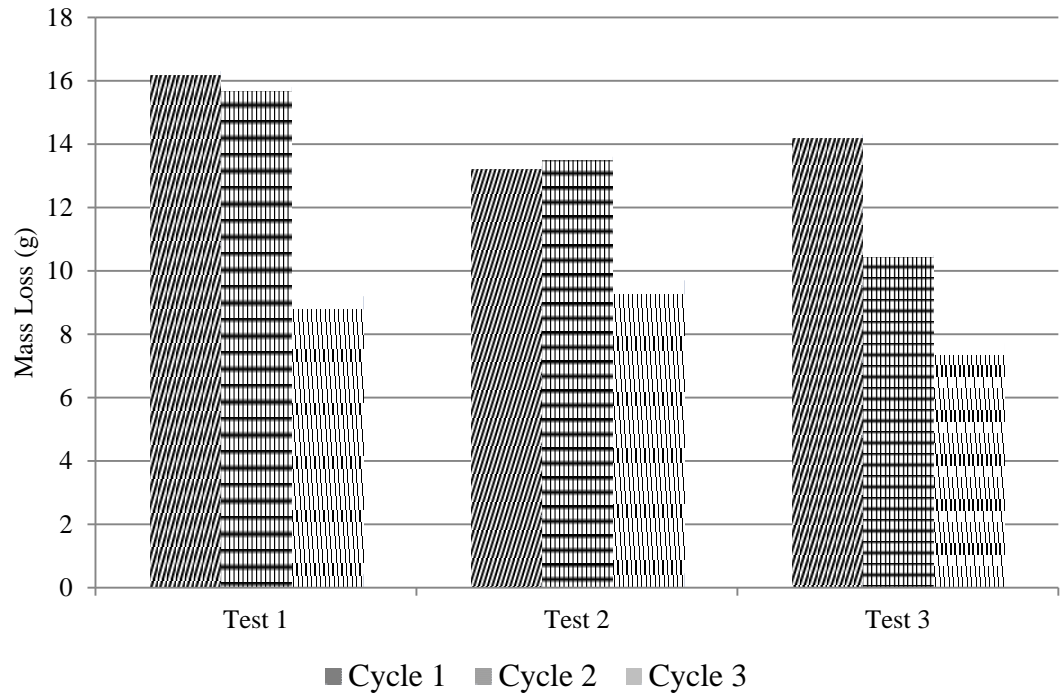


Figure 3.9 - HVFA-H Mass Loss Results

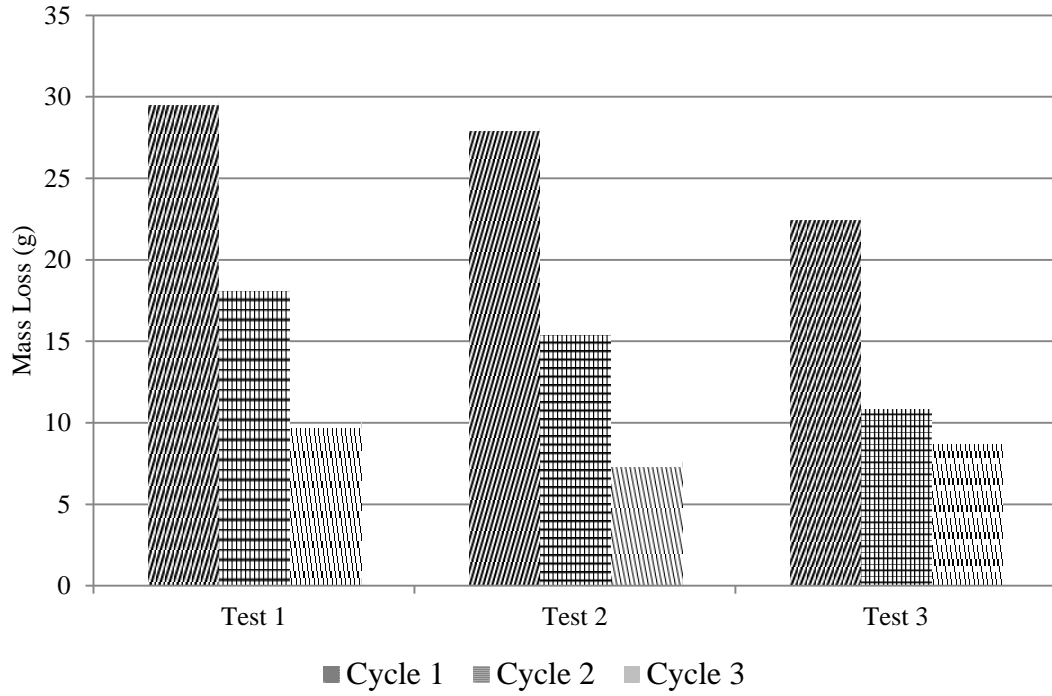


Figure 3.10 - HVFA-L Mass Loss Results

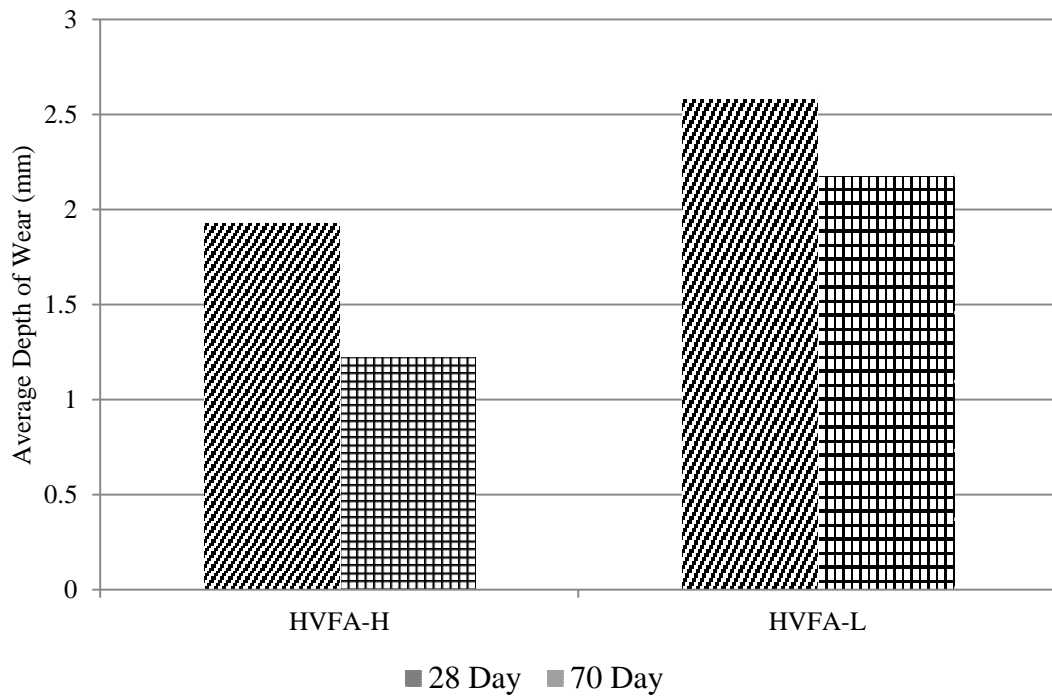


Figure 3.11 - HVFA Average Depth of Wear by Age

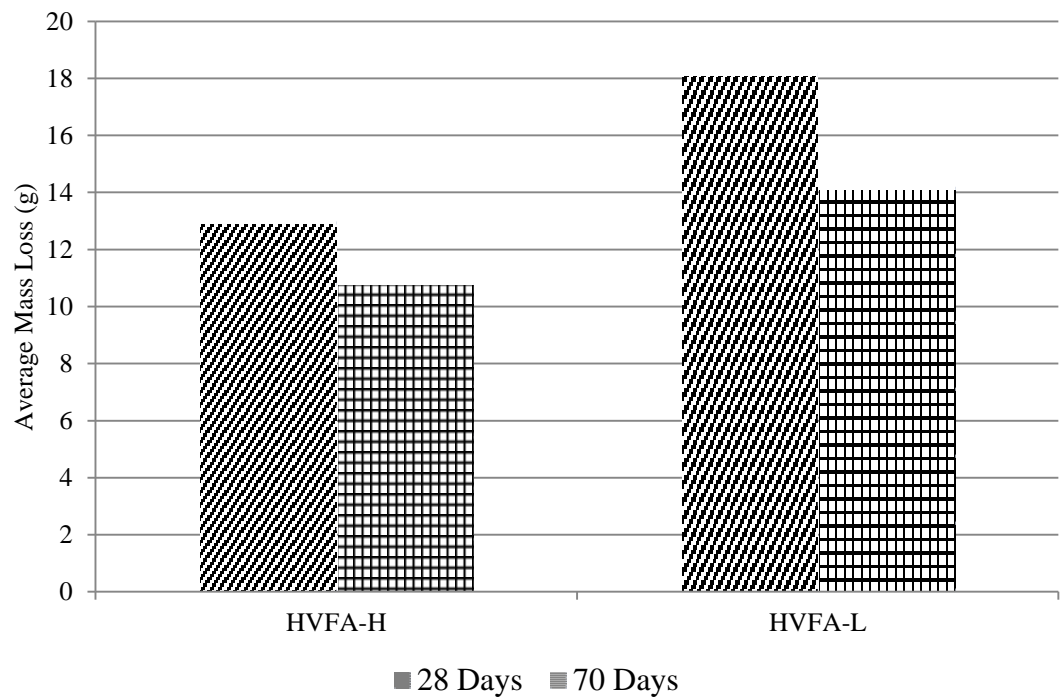


Figure 3.12 - HVFA Average Mass Loss by Age

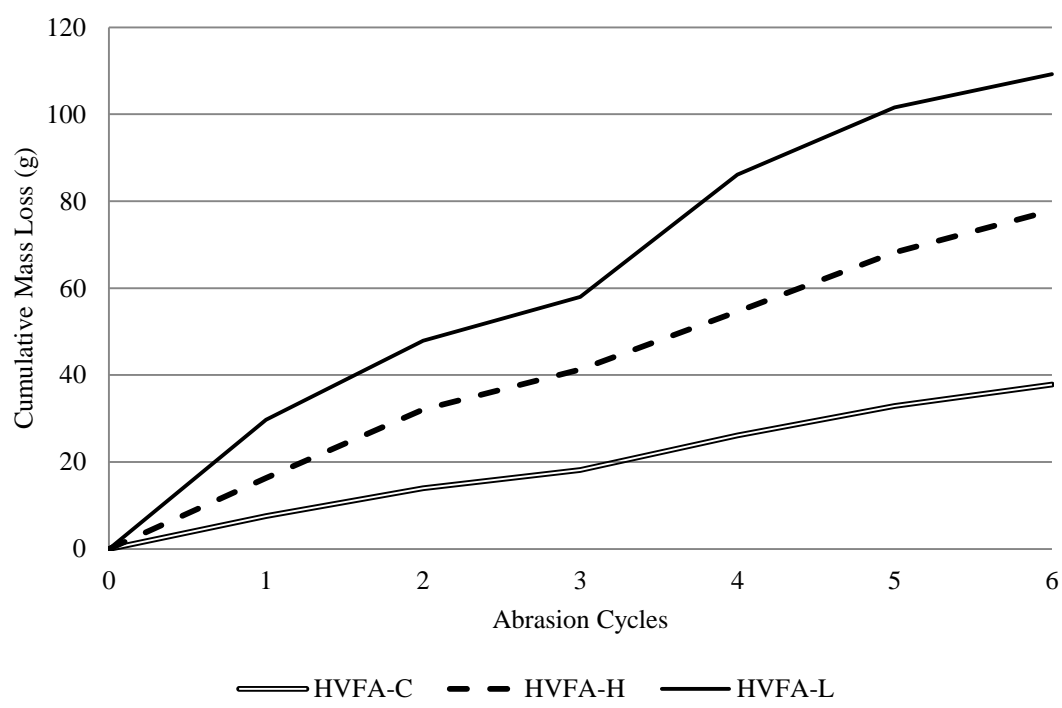


Figure 3.13 - HVFA Mass Loss Results

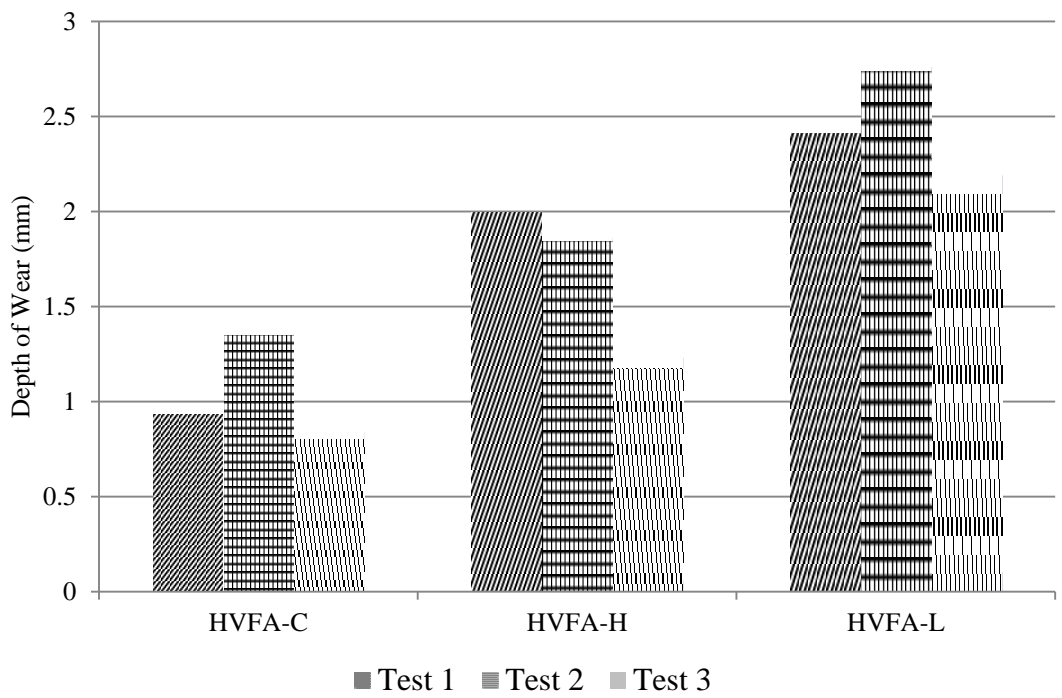


Figure 3.14 - HVFA Depth of Wear Results

Table 3.2 - Average Mass Loss Shown with 28 Day Compressive Strength

	HVFA-C	HVFA-H		HVFA-L	
28 Day Compressive Strength (psi)	5,400	3,100		3,500	
Age (days)	28	28	70	28	70
Avg. Mass Loss (g)	6.06	12.98	10.83	18.2	14.2
Avg. Depth of Wear (mm)	1.05	1.94	1.23	2.60	2.19

Conversion: 1 MPa = 145.04 psi
 1 lb. = 453.59 g
 1 in. = 25.4 mm

3.3.2. Discussion and Conclusions. Results are very consistent with findings by both Naik and Atis. The compressive strength of the concrete seems to have the most influence on its abrasion resistance. The two HVFA concrete mixes showed

significantly less resistance to abrasion than HVFA-C. This can be attributed to the lower compressive strengths of the HVFA concrete relative to the control. When comparing the two HVFA concrete mixes to each other, however, compressive strength does not seem to be as indicative of abrasion resistance. The results suggest that at identical levels of fly ash replacement, abrasion resistance is more affected by volume of cementitious material rather than compressive strength, however more testing is warranted to confirm this conclusion. Because the lower relative resistance to abrasion of HVFA concrete is most likely due to its strength, and not necessarily the fly ash replacement level, it is difficult to make conclusive findings on the effect of fly ash replacement on abrasion resistance without a larger scale investigation. As shown in **Figures 3.10 -3.11**, the abrasion resistance of both HVFA concrete mixes did increase with age. This suggests that, at later ages when HVFA concrete reaches improved strength, its abrasion resistance could be similar to that of conventional concrete, although further testing would be needed.

APPENDIX A
SHRINKAGE DATA WITH RELATIVE HUMIDITY DATA

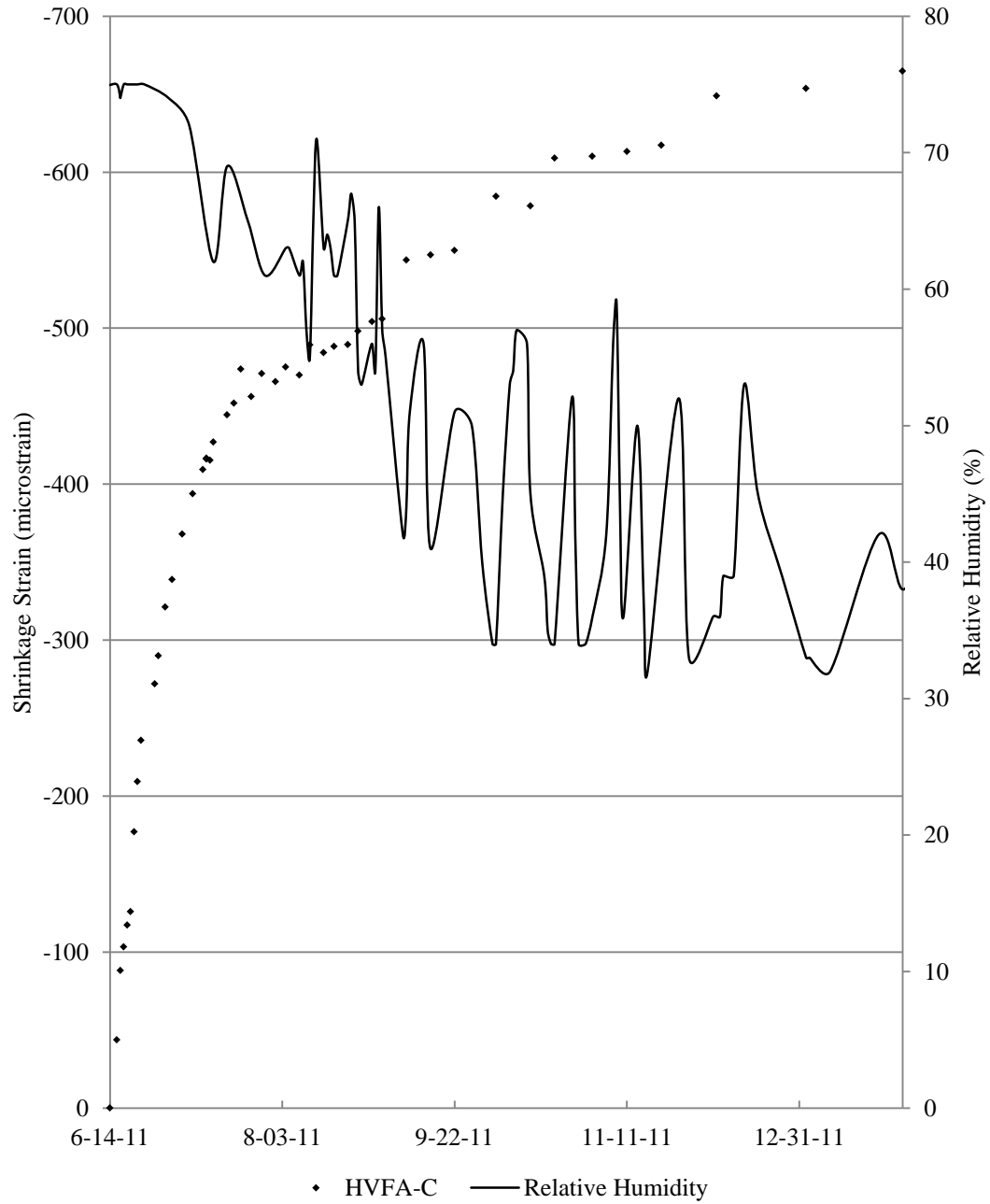


Figure A.1 – HVFA-C shrinkage data shown with recorded relative humidity

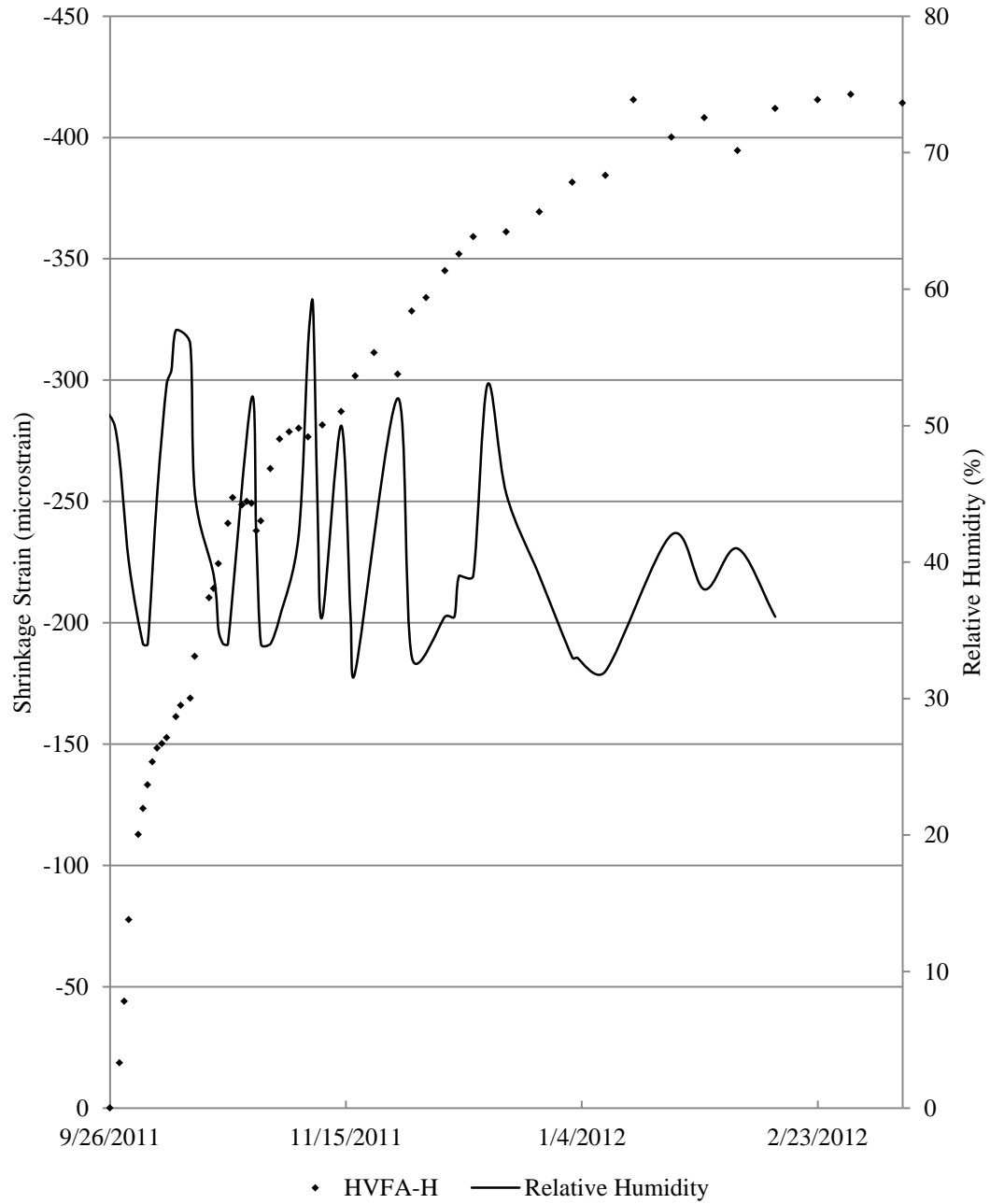


Figure A.2 – HVFA-H shrinkage data shown with recorded relative humidity

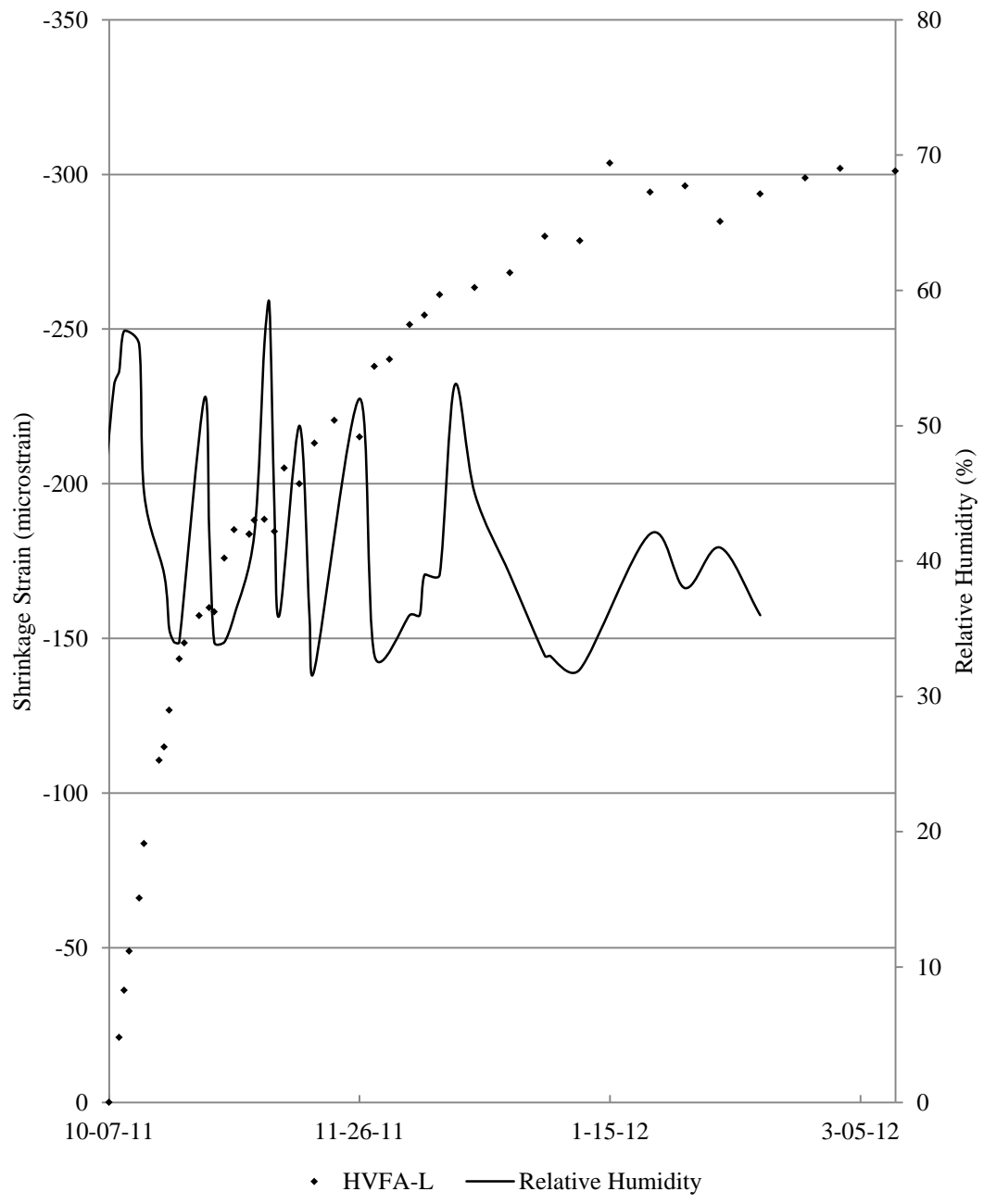


Figure A.3 – HVFA-L shrinkage data shown with recorded relative humidity

APPENDIX B
EXAMPLE STRAIN CALCULATIONS

	A	B	C	D	E	F	G
1			Example Shrinkage and Creep Calculation				
2							
3			G= 0.40 x 10 ⁻⁵ (mm/mm)				
4			G= 4.00 x 10 ⁻⁶ (mm/mm)				
5							
6					Measured Data		
7			Specimen	Reading			
8			Refer Bar		2525	2524	2525
9			C6-58L SH1	1--1	2130	2111	2106
10			C6-58L SH1	1--2	3633	3615	3611
11			C6-58L SH1	1--3	4018	4002	3998
12			C6-58L SH1	2--1	2549	2531	2529
13			C6-58L SH1	2--2	3179	3162	3162
14			C6-58L SH1	2--3	3230	3213	3210
15			C6-58L SH1	3--1	5867	5846	5846
16			C6-58L SH1	3--2	1980	1962	1960
17			C6-58L SH1	3--3	2182	2166	2165
18							
19							
20					Calculated Strain		
21							
22			C6-58L SH1	1--1		-72	-24
23			C6-58L SH1	1--2		-68	-20
24			C6-58L SH1	1--3		-60	-20
25			C6-58L SH1	2--1		-68	-12
26			C6-58L SH1	2--2		-64	-4
27			C6-58L SH1	2--3		-64	-16
28			C6-58L SH1	3--1		-80	-4
29			C6-58L SH1	3--2		-68	-12
30			C6-58L SH1	3--3		-60	-8
31							
32			Average Shrinkage			-67.1	-13.3
33			Cumulative Shrinkage			-67.1	-80.4
34							

Figure B.1 – Example shrinkage and creep strain calculation

	A	B	C	D	E	F	G
1			Example Shrinkage and Creep Calculation				
2							
3			G= 0.4 x 10 ⁻⁵ (mm/mm)				
4			G= 4 x 10 ⁻⁶ (mm/mm)				
5							
6						Measured Data	
7			Specimen	Reading			
8			Refer Bar		2525	2524	2525
9			C6-58L SH1	1--1	2130	2111	2106
10			C6-58L SH1	1--2	3633	3615	3611
11			C6-58L SH1	1--3	4018	4002	3998
12			C6-58L SH1	2--1	2549	2531	2529
13			C6-58L SH1	2--2	3179	3162	3162
14			C6-58L SH1	2--3	3230	3213	3210
15			C6-58L SH1	3--1	5867	5846	5846
16			C6-58L SH1	3--2	1980	1962	1960
17			C6-58L SH1	3--3	2182	2166	2165
18							
19							
20						Calculated Strain	
21							
22			C6-58L SH1	1--1		=B54*((F9-E9)-(F58-E58))	=B54*((G9-F9)-(G58-F58))
23			C6-58L SH1	1--2		=B54*((F10-E10)-(F58-E58))	=B54*((G10-F10)-(G58-F58))
24			C6-58L SH1	1--3		=B54*((F11-E11)-(F58-E58))	=B54*((G11-F11)-(G58-F58))
25			C6-58L SH1	2--1		=B54*((F12-E12)-(F58-E58))	=B54*((G12-F12)-(G58-F58))
26			C6-58L SH1	2--2		=B54*((F13-E13)-(F58-E58))	=B54*((G13-F13)-(G58-F58))
27			C6-58L SH1	2--3		=B54*((F14-E14)-(F58-E58))	=B54*((G14-F14)-(G58-F58))
28			C6-58L SH1	3--1		=B54*((F15-E15)-(F58-E58))	=B54*((G15-F15)-(G58-F58))
29			C6-58L SH1	3--2		=B54*((F16-E16)-(F58-E58))	=B54*((G16-F16)-(G58-F58))
30			C6-58L SH1	3--3		=B54*((F17-E17)-(F58-E58))	=B54*((G17-F17)-(G58-F58))
31							
32			Average Shrinkage			=AVERAGE(F22:F30)	=AVERAGE(G22:G30)
33			Cumulative Shrinkage			=F32	=F33+G32
34							
35							

Figure B.2 – Example shrinkage and creep strain calculations with equations shown

APPENDIX C
COEFFICIENT OF VARIATION DATA

HVFA-C		Shrinkage														
Age (days)		2	3	4	5	6	7	8	9	13	14	16	18	21	24	27
COV		0.14	0.20	0.57	0.41	1.66	0.34	0.33	0.34	0.31	0.38	0.22	0.20	0.17	0.21	0.51
		28	29	30	34	36	38	41	44	48	51	55	58	62	65	69
		0.57	0.44	0.41	0.37	0.32	0.30	0.52	0.32	0.47	0.31	0.49	0.21	0.61	7.27	3.11
		72	76	79	86	93	100	112	122	129	140	150				
		0.34	0.34	0.36	1.48	1.69	0.20	0.13	0.43	0.10	0.36	0.36				
		Creep														
Age (days after loading)					1	2	6	8	10	13	16	20	23	27	30	34
COV					0.44	0.41	0.37	0.32	0.30	0.52	0.32	0.47	0.31	0.49	0.21	0.61
		37	41	44	48	51	58	65	72	84	94	101	112	122		
		7.27	3.11	0.34	0.34	0.36	1.48	1.69	0.20	0.13	0.43	0.10	0.36	0.36		
		HVFA-H														
		Shrinkage														
Age (days)		2	3	4	6	7	8	9	10	11	12	14	15	17	18	21
COV		0.46	0.22	0.15	0.19	0.37	0.39	0.42	0.54	1.29	1.13	0.42	0.60	1.07	0.16	0.20
		22	23	25	26	28	29	30	31	32	34	36	38	40	42	45
		1.03	0.38	0.47	0.60	1.17	3.09	4.24	0.14	1.50	0.23	0.24	1.04	2.36	0.94	0.77
		49	52	56	61	64	67	71	74	77	84	91	98	105	111	119
		0.75	0.21	0.36	0.40	0.23	1.08	0.26	0.33	0.36	1.97	0.49	0.31	1.63	0.16	0.24
		126	133	141	150											
		0.34	0.15	0.27	1.01											
		Creep														
Age (days after loading)					1	2	3	4	6	8	10	12	14	17	21	24
COV					0.49	0.81	0.90	0.31	0.25	0.22	0.51	1.31	0.67	0.33	0.37	0.30
		28	33	36	39	43	46	49	56	63	70	77	83	91	98	105
		0.21	0.66	0.21	0.35	0.16	0.25	0.30	0.36	0.26	0.19	0.21	0.10	1.59	1.08	5.28
		113	122													
		0.21	0.24													

Figure C.1 – HVFA-C and HVFA-H COV Data

HVFA-L		Shrinkage														
Age (days)		2	3	4	6	7	10	11	12	14	15	18	20	21	23	25
COV		0.25	0.27	0.35	0.29	0.16	0.15	0.57	0.26	0.22	0.67	0.42	0.83	2.88	0.19	0.36
		28	29	31	33	35	38	41	45	50	53	56	60	63	66	73
		1.70	0.47	10.22	0.78	0.13	0.36	0.37	0.47	0.37	0.24	2.45	0.25	0.54	0.39	1.64
		80	87	94	100	108	115	122	130	139	146	157				
		0.66	0.25	2.09	0.24	0.81	1.52	0.19	0.26	0.48	0.54	1.99				

		Creep														
Age (days after loading)					1	3	5	7	10	13	17	22	25	28	32	35
COV					0.56	0.37	0.37	0.28	0.66	0.24	0.21	0.47	0.37	0.40	0.17	0.55
		38	45	52	59	66	72	80	87	94	102	111	118	129		
		0.55	0.30	0.19	0.24	0.34	0.15	1.87	0.53	6.72	0.22	2.53	5.17	1.43		

Figure C.2 – HVFA-L COV Data

BIBLIOGRAPHY

- Alexander, K.M., Wardlaw, J., and Ivanusec, I. (1986). "A 4:1 Range in Concrete Creep When Cement SO₃ Content, Curing Temperature and Fly Ash Content are Varied." *Cement and Concrete Research*, Vol. 16, 173-180.
- American Coal Ash Association (ACAA) (2010). "2010 Coal Combustion Product (CCP) Production & Use Survey Report." ACAA, Aurora, Colorado.
- American Concrete Institute (ACI 116R-00) (2000), "Cement and Concrete Terminology." American Concrete Institute, Detroit, Michigan.
- American Concrete Institute (ACI 209R-92) (1997), "Prediction of Creep, Shrinkage, and Temperature Effects in Concrete Structures." American Concrete Institute, Detroit, Michigan.
- American Concrete Institute (ACI 209.1R-05) (2005), "Report on Factors Affecting Shrinkage and Creep of Hardened Concrete." American Concrete Institute, Detroit, Michigan.
- American Concrete Institute (ACI 232.2R-03) (2003), "Use of Fly Ash in Concrete." American Concrete Institute, Detroit, Michigan.
- American Concrete Institute (ACI 318-08) (2008), "Building Code Requirements for Structural Concrete and Commentary." American Concrete Institute, Detroit, Michigan.
- ASTM C31/C31 M-09 (2009). "Standard Practice for Making and Curing Concrete Test Specimens in the Field." American Society for Testing and Materials, West Conshohocken, Pennsylvania.
- ASTM C39/C39 M-05 (2005). "Standard Test Method for Compressive Strength of Cylindrical Concrete Specimens." American Society for Testing and Materials, West Conshohocken, Pennsylvania.
- ASTM C157/C157 M-08 (2008). "Standard Practice for Length Change of Hardened Hydraulic-Cement Mortar and Concrete." American Society for Testing and Materials, West Conshohocken, Pennsylvania.
- ASTM C3512/C512 M-10 (2010). "Standard Practice for Creep of Concrete in Compression." American Society for Testing and Materials, West Conshohocken, Pennsylvania.

- ASTM C944/C944 M-99 (2005). "Standard Practice for Abrasion Resistance of Concrete of Mortar Surfaces by the Rotating-Cutter Method." American Society for Testing and Materials, West Conshohocken, Pennsylvania.
- Atis, C.D. (2002). "High Volume Fly Ash Abrasion Resistant Concrete." *Journal of Materials in Civil Engineering*, May/June 2002, 274-277.
- Atis, C.D. (2003). "High-Volume Fly Ash Concrete with High Strength and Low Drying Shrinkage." *Journal of Materials in Civil Engineering*, March/April 2003, 153-156.
- Bazant, Z. P. and Baweja, S. (2000). "Creep and Shrinkage Prediction Model for Analysis and Design of Concrete Structures: Model B3" Adam Neville Symposium: Creep and Shrinkage—Structural Design Effects, ACI SP-194, A.Al-Manaseer, ed., Am. Concrete Institute, Farmington Hills, Michigan, 2000, 1-83.
- Comite Euro – International Du Beton (CEB) (1990), "CEB-FIP Model Code 1990" Thomas Telford, 1990-1993, 53-58.
- Freyermuth, C.L. (1969). "Design of Continuous Highway Bridges with Precast, Prestressed Concrete Girders." *Journal of the Prestressed Concrete Institute*, Vol. 14, No. 2, 14-39.
- Gao, P., et. al. (2006). "Effect of Fly Ash on Deformation of Roller-Compacted Concrete." *ACI Materials Journal*, October 2006, 336-339.
- Gardner, N.J., and Lockman, M.J. (2001), "Design Provisions for Drying Shrinkage and Creep of Normal-Strength Concrete" *ACI Materials Journal*, 159-167.
- Marlay, K.M., (2011). "Hardened Concrete Properties and Durability Assessment of High Volume Fly Ash Concrete." M.S. Thesis, Missouri University of Science and Technology, Rolla, MO.
- Myers, J.J., Carrasquillo, R.L. (1999). "The Production and Quality Control of High Performance Concrete in Texas Bridge Structures," Center for Transportation Research, Report Number 580-589-1, November 1999, pp 564.
- Myers, J.J. and Yang, Y. "High Performance Concrete for Bridge A6130-Route 421 Pemiscot County, MO." UTC R39.
- Naik, T.R., Singh, S.S., and Ramme, B.W. (2002). "Effect of Source of Fly Ash on Abrasion Resistance of Concrete." *Journal of Materials in Civil Engineering*, September/October 2002, 417-426.

- Nath, P. and Sarker, P. (2011). "Effect of Fly Ash on the Durability Properties of High Strength Concrete." *Procedia Engineering*, 14 (2011), 1149-1156.
- Ortega, C.A., (2012). "Shear and Fracture Behavior of High-Volume Fly Ash Reinforced Concrete for Sustainable Construction." PhD Dissertation, Missouri University of Science and Technology, Rolla, MO.
- Perenchio, W.F., (1997). "The Drying Shrinkage Dilemma-Some Observations and Questions About Drying Shrinkage and its Consequence," *Concrete Construction*, V. 42, No. 4, pp. 379-383.
- Tadros, M.K., Al-Omaishi, N., Seguirant, S.J., and Gallt, J.G. (2003). "Prestress Losses in Pretensioned High-Strength Concrete Bridge Girders." National Cooperative Highway Research Program Report 496, Transportation Research Board, National Research Council, Washington, D.C.
- Termkhajornkit, P., et.al. (2005). "Effect of Fly Ash on Autogenous Shrinkage." *Cement and Concrete Research*, 35 (2005), 473-482.
- U.S. Green Building Council (USGBC) (2009). "LEED Reference Guide for Green Building and Construction." USGBC, Washington, D.C., 369-377.